

2014

M.Tech Project Thesis



Axial Conduction in a Partially Heated Microchannel Subjected to Isothermal Boundary Condition

**RAJEEV R PRASAD
ROLL NO 211ME3192**

Under the guidance of

Prof. M.K.Moharana (Supervisor)

Department of Mechanical Engineering
National Institute of Technology Rourkela
Odisha , India - 769 008

A Project Report

on

**Axial conduction in a partially heated microchannel
subjected to isothermal boundary condition**

By

RAJEEV R PRASAD

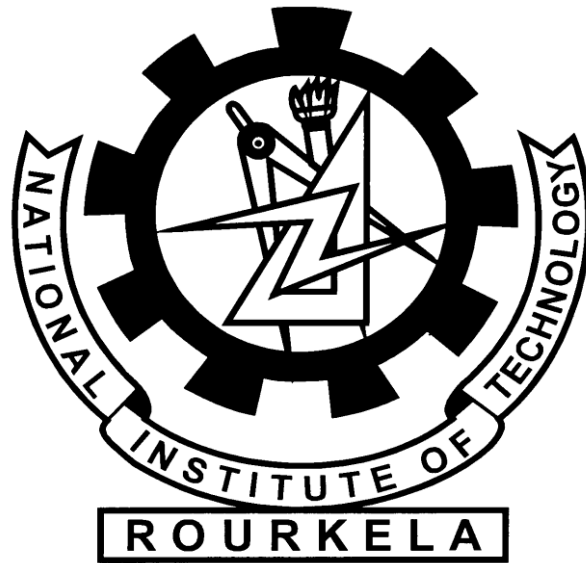
ROLL NO 211ME3192



DEPARTMENT OF MECHANICAL ENGINEERING

NATIONAL INSTITUTE OF TECHNOLOGY

ROURKELA 769008



National Institute of Technology
Rourkela (India)

CERTIFICATE

This is to certify that the report entitled, “**Axial conduction in a partially heated microchannel subjected to isothermal boundary condition**” submitted by **Mr. Rajeev R Prasad** in partial fulfillment of the requirements for the award of Master of Technology in Mechanical Engineering with Thermal Engineering specialization in the Department of Mechanical Engineering, National Institute of Technology Rourkela is an authentic work carried out by him under my supervision and guidance. To the best of my knowledge, the matter embodied in this thesis has not been submitted to any other University/Institute for the award of any Degree or Diploma.

Date:

Dr. Manoj Kumar Moharana
Department of Mechanical Engineering
National Institute of Technology, Rourkela

SELF DECLARATION

I, Mr Rajeev R Prasad, Roll No. 211ME3192, student of M. Tech (2011-14), Thermal Engineering at Department of Mechanical Engineering, National Institute of Technology Rourkela do hereby declare that I have not adopted any kind of unfair means and have carried out the research work reported in this thesis work ethically to the best of my knowledge. If adoption of any kind of unfair means is found in this thesis work at a later stage, then appropriate action can be taken against me including withdrawal of this thesis work.

NIT Rourkela
02 June 2014


Rajeev R Prasad

ACKNOWLEDGEMENTS

First and foremost, praises and thanks to the God, the Almighty, for His showers of blessings throughout my research work to complete the research successfully.

I would like to express my sincere gratitude to my guide **Prof. MANOJ KUMAR MOHARANA** for enlightening me the first glance of research, and for his patience, motivation, enthusiasm, and immense knowledge. His guidance helped me in all the time of research and writing of this thesis. I could not have imagined having a better advisor and mentor for my project work. It was a great privilege and honour to work and study under his guidance. I am extremely grateful for what he has offered me.

Last but not the least; I would like to thank my family, for supporting me spiritually throughout my life and for their unconditional love, moral support and encouragement.

So many people have contributed to my research work, and it is with great pleasure to take the opportunity to thank them.

RAJEEV R PRASAD

ABSTRACT

Thermal management is indispensable for longevity of electronic equipment's. Continuous miniaturization of chips and demand for proper cooling arrangement has paved way for lot of research work on micro channels. Though lot of research has been carried on regarding thermal characterization at micro scale level, there is still much diversion of results to be discerned in the various reports published. One of the possible causes of diversion is axial conduction. A numerical study has been carried out to understand the effects of axial conduction in a conjugate heat transfer situation involving simultaneously developing laminar flow and heat transfer in a square micro channel subjected to isothermal boundary conditions at bottom of substrate while the other exposed surfaces are kept insulated. Generally ends of the micro tubes are insulated because of demand of physical situation. Taking this constraint into account study is carried out for different partial heating cases also. Different cases considered for this work are : (i) The entire bottom surface of micro channel is subjected to isothermal boundary condition while all other outer surfaces are insulated (ii) 6 mm of bottom surface is insulated from both inlet and outlet end of micro channel and remaining length of bottom surface is subjected to isothermal boundary condition (iii) 6 mm of bottom surface is insulated from inlet end of micro channel and remaining length of bottom surface is subjected to isothermal boundary condition (iv) 6 mm of bottom surface is insulated from outlet end of micro channel and remaining length of bottom surface is subjected to isothermal boundary condition. Simulations are carried out for different conductivity ratio, Reynolds number and substrate thickness to channel depth. It is found that value of Nu_{avg} is increasing with decreasing value of k_{sf} upto k_{sf} approximately equal to 25 and beyond that on decreasing k_{sf} value further, value of Nu_{avg} starts decrease rapidly. This sudden decrease in Nu_{avg} value is because under such situation the case becomes a one side heating problem rather than three sided heating problem. Now as k_{sf} is increased beyond a range axial back conduction comes into play and this causes value of Nu_{avg} to decrease. Thus, there exists an optimum k_{sf} for which Nu_{avg} is maximum for given flow Re and wall thickness ratio. Secondly, it is observed that higher axial conduction causes the boundary condition experienced at the solid fluid interface to drift more towards iso-flux condition although isothermal condition is applied on outer surface.

Keywords : Axial conduction, Conjugate heat transfer, Microchannel.

TABLE OF CONTENTS

Title	Page No.
ACKNOWLEDGEMENTS	i
ABSTRACT	ii
CONTENTS	iii
LIST OF FIGURES	iv
LIST OF TABLE	vi
NOMENCLATURE	vii
GREEK SYMBOLS	vii
SUBSCRIPTS	vii
1. INTRODUCTION	1
1.1 What is axial back conduction?	1
1.2 What are characteristics of Micro size channels ?	3
2. LITERATURE REVIEW	4
3. NUMERICAL ANALYSIS	9
3.1 Introduction	9
3.2 Grid independence test	13
3.3 Data reduction	13
4. RESULTS AND DISCUSSION	15
5. CONCLUSIONS	33
6. REFERENCES	35

LIST OF FIGURES

No:	Table	Page
1.1	Variation of bulk fluid and local wall temperature in the flow direction of a circular duct subjected to (a) constant wall heat flux (b) constant wall temperature.	2
1.2	Cross-sectional view of microtube.	3
3.1	Simulated domain details.	10
3.2	Four different cases of heating the microchannel on its outer surface with constant wall temperature condition while keeping all other faces insulated (a) Heating over full length of microchannel substrate base (b) 6 mm insulated near inlet and outlet of bottom wall of the substrate (c) 6 mm insulated near inlet of bottom wall of the substrate (d) 6 mm insulated near outlet of bottom wall of the substrate.	11
3.3	Axial variation of local Nusselt number for $\delta_s = 0$ for three different mesh sizes.	13
4.1	Axial variation of dimensionless wall temperature and bulk fluid temperature as a function of δ_{sf} , k_{sf} and Re (for heating as per Case-1).	16
4.2	Axial variation of dimensionless wall temperature and bulk fluid temperature as a function of δ_{sf} , k_{sf} and Re (for heating as per Case-2).	17
4.3	Axial variation of dimensionless wall temperature and bulk fluid temperature as a function of δ_{sf} , k_{sf} and Re (for heating as per Case-3).	18
4.4	Axial variation of dimensionless wall temperature and bulk fluid temperature as a function of δ_{sf} , k_{sf} and Re (for heating as per Case-4).	19
4.5	Axial variation of dimensionless heat flux as a function of δ_{sf} , k_{sf} and Re (for heating as per Case-1).	20
4.6	Axial variation of dimensionless heat flux as a function of δ_{sf} , k_{sf} and Re (for heating as per Case-2).	21
4.7	Axial variation of dimensionless heat flux as a function of δ_{sf} , k_{sf} and Re (for heating as per Case-3).	22
4.8	Axial variation of dimensionless heat flux as a function of δ_{sf} , k_{sf} and Re (for heating as per Case-4).	23

4.9	Axial variation of local Nusselt number as a function of δ_{sf} , k_{sf} and Re (for heating as per Case-1).	24
4.10	Axial variation of local Nusselt number as a function of δ_{sf} , k_{sf} and Re (for heating as per Case-2).	25
4.11	Axial variation of local Nusselt number as a function of δ_{sf} , k_{sf} and Re (for heating as per Case-3).	26
4.12	Axial variation of local Nusselt number as a function of δ_{sf} , k_{sf} and Re (for heating as per Case-4).	27
4.13	Variation of average Nusselt number with k_{sf} for Re = 100-500 and $\delta_{sf} = 1-5$ for different cases of heating the microchannel.	28
4.14	Temperature contours for Case 1(Heating over full length of microchannel substrate base).	29
4.15	Temperature contours for Case 2 (6 mm insulated near inlet and outlet of bottom wall of the substrate).	30
4.16	Temperature contours for Case 3 (6 mm insulated near inlet of bottom wall of the substrate).	31
4.17	Temperature contours for Case 4 (6 mm insulated near outlet of bottom wall of the substrate).	32

LIST OF TABLES

No:	Titles	Page no:
1	Different materials considered for the study.	10

Nomenclature

c_p	Specific heat (J/kgK)
D_h	Hydraulic diameter (m)
h_z	Local heat transfer coefficient (W/m ² K)
k_s	Solid thermal conductivity (W/mK)
k_f	Fluid thermal conductivity (W/mK)
k_{sf}	Wall to fluid thermal conductivity ratio (-)
L	Total length of tube (m)
Nu_z	Local Nusselt number (-)
Nu_{avg}	Average Nusselt number (-)
Nu_{fd}	Nusselt number for fully developed flow (-)
Pr	Prandtl number (-)
q_z	Heat at any location z (W/m ²)
q^*	Ratio of heat flux acting at substrate bottom and conjugate wall area (-)
Re	Reynolds number (-)
T_f	Bulk fluid temperature (K)
T_w	Wall temperature (K)
u	Velocity in the axial direction (m/s)
\bar{u}	Average velocity at inlet (m/s)
z^*	Non dimensional axial coordinate (-)

Greek symbols

δ_f	Height of the microchannel (mm)
δ_s	Thickness of the substrate below the microchannel (mm)
δ_{sf}	Ratio of δ_s and δ_f (-)
∇	Differential parameter
μ	Dynamic viscosity (Pas)
ρ	Density (kg/m ³)
ϕ	Non-dimensional heat flux (-)
Θ	Non-dimensional temperature (-)
ω_s	Channel width (mm)

Subscripts

f	Fluid
s	Solid
Z	Axial coordinate

Chapter 1

Introduction

Circuit temperature is one of the major parameters affecting the performance of silicon integrated circuits. Studies suggest that temperature of the circuit should be maintained as low as possible for better performance and longevity of chip. Conventionally, air is used as the coolant. Technological advancements in electronic industry have led to miniaturization of chips and these developments have brought need for high-performance and space-efficient heat dissipating devices. Air cooling no longer remains a feasible option due to its inferior properties like low specific heat and low heat transfer coefficient paving way for more compact heat dissipating devices.

With developments in micromachining technology, many applications in the field of thermal-fluid engineering developed. Some typical applications of micromachining in the field of thermal engineering can be found in Khandekar and Moharana [1]. Tuckerman and Pease [2] had demonstrated that micro channels provide an ideal solution for high heat flux problem caused by electronic devices of miniature size. Microchannels provide a higher heat removal rate than a conventional size channel due to its higher surface area per unit volume paving way for their widespread use in cooling of the electronics.

The study of microchannel liquid cooling techniques has become an attractive research topic and research works conducted over a period of time have identified axial back conduction to play a very critical role in the micro scale heat exchange device performance. Realising the significance of axial back conduction in a micro scale heat exchange device, the present study is focused on its role in heat transfer and provides (i) an in-depth review of research works done so far on this topic (ii) numerical study of axial wall conduction in partially heated microchannels.

1.1 What is axial back conduction?

Consider laminar flow through a circular pipe subjected to constant heat flux boundary condition. Conventionally it is considered that heat applied on the pipe outer surface, flows in radial direction by means of conduction along the solid wall and on reaching the solid- fluid interface, the heat is then carried away by the fluid in the flow direction. The bulk temperature of the fluid is observed to increase in a linear manner in the flow direction because of the continuous addition of heat to fluid. Beyond the thermally developing zone, the duct wall temperature also increases linearly in the direction of flow because the heat transfer coefficient is constant in this region. This analysis is based on assumption that the fluid properties remain constant throughout the flow. Such a

phenomenon is shown in Fig. 1.1(a) where the bulk fluid temperature and the duct wall temperature are varying in the axial direction. It can be seen from Fig. 1.1 (b) that if flow is subjected to isothermal boundary condition on its outer surface, then axial variation of bulk fluid temperature is nonlinear and it approaches asymptotically equal to the wall temperature far away from the inlet.

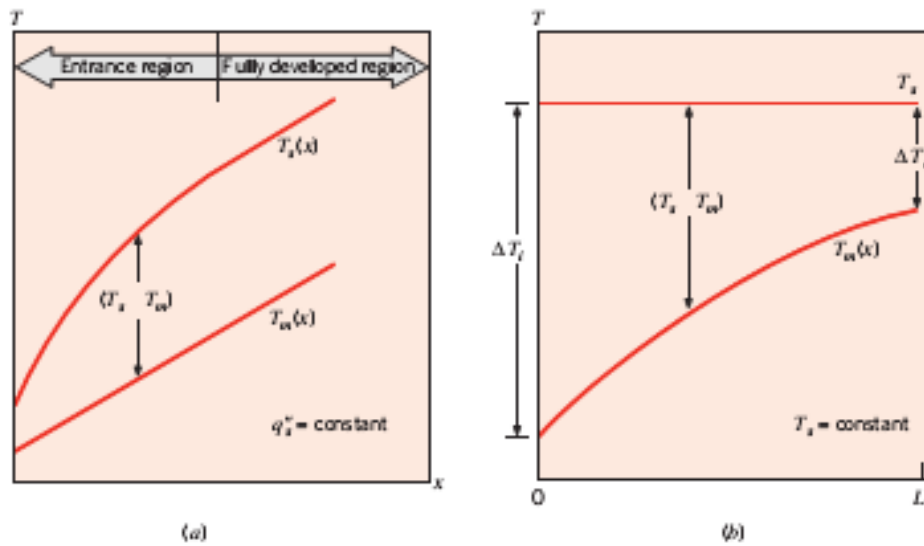


Fig. 1.1: Variation of bulk fluid and local wall temperature in the direction of flow of a circular duct subjected to (a) Constant heat flux (b) Constant wall temperature (Incropera et al. [3]).

It is to mention that duct wall is of finite thickness, therefore the heat flux applied on the outer surface gets conducted radially towards centre of tube and on reaching the inner surface of tube, and it is carried by the fluid in the flow direction.

From Fig. 1.1 (a) it can be noticed that temperature is not uniform along the axial direction both in solid and fluid medium and the maximum temperature is between the inlet & outlet of heated duct. Due to this temperature gradient there is a chance for heat conduction axially along the solid and also along the fluid in a direction opposite to flow direction. Such a phenomenon is called “*axial back conduction*” and it leads to conjugate heat transfer. From Fig. 1.1 (b), it can be noticed that there is no temperature gradient in the axial direction if duct is subjected to isothermal boundary condition. This makes us to think that under such condition there will not be any axial heat conduction, but this needs to be confirmed from the present work.

1.2 What are characteristics of micro size channels?

The solid wall thickness of micro channels are normally of the same order or larger than channel diameter. Fig. 1.2 shows photograph of a micro tube. It can be observed that as the inner diameter of tube is decreased, the relative wall thickness starts to increase.

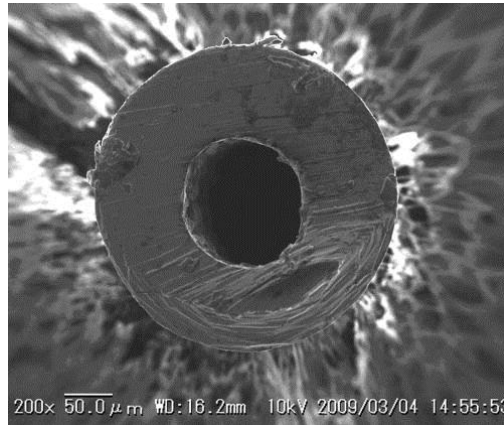


Fig.1.2: Cross sectional view of a microtube (Hong et al. [4]).

As the hydraulic diameter of microchannel decreases, axial back conduction becomes more and more significant. Therefore it is important to identify those thermo-fluidic parameters and to identify those parameters and their influence on heat transfer a numerical analysis is carried out in a partially heated microchannel subjected to isothermal condition on its substrate base. A wide range of thermal conductivity, wall thickness and Reynolds's number are considered for this investigation which is given in detail in chapter 3.

Chapter 2

Literature review

Tuckerman and Pease [2] was the first to introduce the concept of micro channel heat sink and demonstrated that chips can be cooled by means of forced convective flow of water through micro channels. A rectangular micro-channel having a channel width of 50 microns and depth of 302 microns was fabricated in a silicon wafer. It had a capacity to dissipate 790 W/cm^2 and without undergoing any phase change the temperature of substrate could rise as high as 71°C above temperature of water inlet. This was a giant leap in the field of cooling technology.

Philips [5] did thermal and fluid performance test on a micro channel fabricated with Indium phosphide substrate and observed that thermal performance of micro channel is approximately two orders of magnitude better than air cooling.

Peng and Peterson [6] conducted numerical studies in rectangular micro channels using water and found that heat transfer for fluid flowing in a micro channel structure is a function of aspect ratio and the ratio of hydraulic diameter to centre to centre micro channel distance. Adams et al. [7] investigated single phase flows in circular micro channels using water and found that Nu numbers encountered in micro channels are larger in value in comparison to that encountered in macro channels.

Since then, micro channels have received considerable attention and several studies were carried out to optimize the size of the heat sink. For developing an optimization design scheme, an analytical model of the transfer process in the heat sink is required. Heat transfer taking place inside heat sink is a conjugated problem consisting of both conduction and convection mode. Therefore, it is difficult to propose an analytical solution for the energy equation due to complicated nature of flow happening in heat sink. Hence most of the analyses were done using classic fin model in which solid walls are modelled as thin fins and the problem is further simplified by assuming it to be one dimensional heat transfer process having constant heat transfer coefficient and uniform fluid temperature. Though classic fin model provides an easy method to explain a micro channel's heat transfer performance, its accuracy is on the lower end because of numerous assumptions made.

Kim and Kim [8] analysed the axial conduction effect for both circular and rectangular geometries and observed that as aspect ratio and thermal conductivity ratio increases, fluid temperature is found to approach solid temperature.

Fedorov and Viskanta [9] carried out analysis to study the effect of back conduction in a micro channel heat sink and found that thermal resistance decreases with flow Re and reaches an asymptote at higher flow Re.

Ryu et al. [10] carried out a three dimensional numerical analysis on a rectangular cross section micro channel. The objective of this study was to minimize the thermal resistance to predict its thermal behaviour accurately. They assumed top surface of the domain to be adiabatic and applied uniform heat flux on bottom surface of substrate attached to heat generating component while flow through micro channel was assumed to be thermally fully developed to impose the condition of vanishing stream wise diffusion at the outlet. The geometric parameters such as channel depth, channel width and channel number were chosen as design variables and using random search technique channel shape was optimized to maximize the performance of micro channel. Derivatives of the governing equation was then discretised using central differencing scheme except for the convective terms which was done by upwind scheme and the discretised equations were then solved using ADI-type-finite-volume method. From their investigation it was found that channel width is the most crucial quantity among the various design variables in deciding the performance of micro channel heat sink. Also no appreciable change in optimal channel shape was noticed when the variations in channel number were large and optimal dimensions were observed to have a power law dependence on pumping power.

Toh et al. [11] carried out a detailed numerical analysis on the experimental conditions of Tuckerman and Pease [2] using finite volume method and found that pressure drop or frictional losses decrease when heat is added compared to adiabatic fluid flow. This is due to decrease in viscosity of working fluid as its temperature increases on addition of heat.

Qu and Mudawar [12] carried out experiments on a micro channel heat sink having a channel of width 231 microns and depth 712 microns to study pressure drop and heat transfer. They solved conjugate heat transfer problem analytically also by treating both the fluid and solid as a unitary computational domain and they found that heat flux and Nusselt number have higher value near inlet and vary around the periphery with Nusselt number approaching zero near the corners.

Upadhye and Kandlikar [13] performed experiment on a chip with 25 mm × 25 mm active cooling surface area covered with micro channels and heat dissipating devices respectively

on either sides for two boundary conditions: isoflux and isothermal. They observed that wide and shallow channel is inferior to a narrow and deep channel from both heat transfer perspective and pressure drop perspective. In addition to this, they also observed that pressure drop for isoflux boundary condition is higher than pressure drop for constant temperature case.

Hetsroni et al. [14] carried out experimental investigations on single phase heat transfer in laminar flow regime ($Re = 95-774$) for a micro tube placed inside a vacuum chamber and subjected to constant heat flux. The Nusselt number was observed to increase with Reynolds number at very low Reynolds number ($10 < Re < 100$) but the increase in Re was less for higher Reynolds number. They concluded that axial conduction is responsible for such behaviour. For $Re > 150$ and $M < 0.01$, they concluded that heat transfer taking place through substrate becomes negligible and both at inlet and outlet adiabatic conditions can be imposed while for $Re < 150$ and $M > 0.01$ heat transfer taking place through substrate is substantial.

Yang and Lin [15] studied the heat transfer characteristics of water in micro channels by using non-intrusive liquid crystal thermography and found that transition occurs at Reynolds number 2300-3000. They also found that the thermal entrance length in microtube is longer than the value normally calculated using the conventional correlation. Lelea [16] studied the effect of the heating position on thermal & hydrodynamic behaviour of micro channel and observed that partial heating strongly influences the characteristics of micro channel.

Zhang et al. [17] investigated the effect of axial heat conduction using finite volume method in a conjugate heat transfer problem and found that the dimensionless heat flux at the solid-fluid interface becomes uniform when back conduction becomes substantial.

Satapathy [18] analytically solved steady state heat transfer problem for a two dimensional laminar rarefied gas flow through a micro channel using separation of variable method. The author concluded that both local Nusselt number and local bulk mean temperature is directly proportional to Peclet number but inversely proportional to Knudsen number.

Hasan [19] did numerical study to investigate the effect of axial conduction and entrance region on internal forced convection in a rectangular channel, and observed that axial conduction is reasonably large in entrance region and increasing the length of entrance region increases the axial conduction while length of channel have no influence on axial conduction.

Moharana et al. [20] analysed both experimentally and numerically axial conduction in single phase simultaneously developing flow through a rectangular mini channel array and found that for higher axial conduction number (M), Nusselt number obtained is smaller than the value given by numerical model.

Rahimi and Mehryar [21] studied the effect of axial heat conduction on local Nusselt number at the entrance and ending region of micro channel. They observed that axial conduction causes a drop in Nusselt number value at the entrance region and a considerable deviancy in value of Nusselt number from fully developed value at the ending region of micro channel.

Moharana and Khandekar [22] studied the effect of axial conduction in a laminar simultaneously developing flow through micro channel subjected to isothermal and iso flux boundary conditions at the outer surface. They found that for constant flux case Nu_{avg} is maximum for an optimum k_{sf} but for isothermal case no such optimum k_{sf} is observed for maximum Nu_{avg} .

Moharana et al. [23] carried out numerical analysis of a square micro channel subjected to constant wall flux only at bottom and insulated from remaining three sides. Based on the analysis they concluded that thermal conductivity ratio plays a significant role in deciding axial conduction and difference between fluid temperature and wall temperature no longer remains constant in fully developed region.

Moharana and Khandekar [24] carried out numerical simulation to study the effect of aspect ratio on heat transfer using a rectangular shaped micro channel subjected to constant flux boundary condition at its bottom face and found that Nu_{avg} is minimum for microchannel aspect ratio 2.

Kumar and Moharana [25] carried out numerical analysis to study the effect of axial conduction in a partially heated microtube and they found that except at low k_{sf} , Nu_{avg} for thicker wall microtube is less than that for thinner wall tube.

Tiwari et al. [26] carried out numerical analysis to study the effect of axial wall conduction in partially heated microtube and found that Nu_{avg} is maximum for an optimum k_{sf} . They also observed that for higher wall thickness, Nu_{avg} is small due to effect of axial wall conduction and Nu_{avg} is increasing with flow Re because of higher thermal development length.

Mishra and Moharana [27] carried out numerical analysis to study the effect of pulsating flow on the axial wall conduction in a microtube subjected to constant heat flux boundary condition on its outer surface and found that there exists an optimum k_{sf} at which overall

Nusselt number is maximum for a particular pulsation frequency (W_0). They also found that pulsation frequency has little effect on heat transfer and for a change in phase angle from 0 to 90, due to increase in instantaneous velocity, heat flux experienced at interface increases resulting in higher heat transfer but for a change in phase angle from 90 to 270 heat flux at interface is observed to decrease.

Although a number of experiments and numerical analysis have been done over these years to understand the role and effects of axial conduction on heat transfer not much is known about scenarios involving partial heating. Keeping this in mind a three dimensional numerical analysis has been carried out to understand axial conduction and its effects on heat transfer in a micro channel subjected to partial heating. The detailed numerical analysis adopted is presented in next chapter.

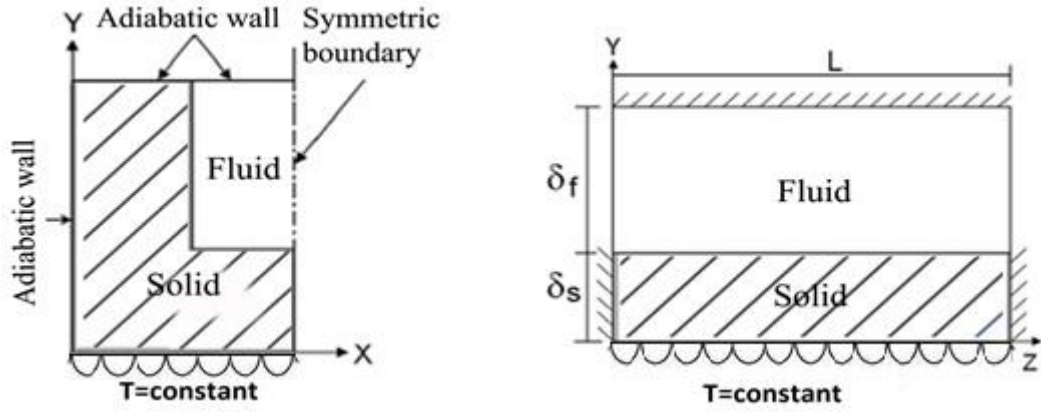


Fig. 3.1: Simulated domain details: (a) Microchannel having conductive wall (b) Cross section of channel (c) Transverse section (Y-Z) plane along the symmetrical plane.

Table 3.1: Different Materials considered for study

Material	Density (kg/m ³)	Sp. Heat (J/kgK)	k _s (W/mK)	k _{sf}
Silicon dioxide	2200	745	1.38	2.26
Bismuth	9780	122	7.86	12.88
Nichrome	8400	420	12	19.66
Constanatan	8920	384	23	37.69
Bronze	8780	355	54	88.48
Aluminium	2700	910	202.38	331.6
Copper	8940	390	387.5	635

The thickness of the substrate below the microchannel is represented as δ_s and height of the microchannel is represented as δ_f . Thus a parameter called δ_{sf} is defined as ratio of δ_s to δ_f . The width (ω_s), depth (δ_f) and length (L) of the channel are maintained constant at 0.4 mm, 0.4 mm and 60 mm respectively. Channels hydraulic diameter (D_h) is obtained as

$$D_h = 4 \left(\frac{\text{Area}}{\text{Perimeter}} \right) = 4 \left(\frac{0.4^2}{4 \times 0.4} \right) = 0.4 \text{ mm.}$$

To understand the influence of substrate thickness on conjugate heat transfer, wall thickness (δ_s) of the microchannel is varied keeping width of substrate constant. Pure water (inlet temperature = 300 K and $Pr \approx 7$) with conductivity k_f is used as working fluid and Re number is varied in the range of 100 to 500. The wall conductivity is also varied in such a way that k_{sf} varies in the range of 2 to 635. It is to be noted that k_{sf} is defined as ratio of k_s and k_f .

Except the bottom face, all the other solid faces of the micro channel are assumed to be insulated. Since it is computationally intensive to carry out the analysis of the whole micro

channel, keeping symmetry in mind for analysis only one half transverse section of the micro channel along the plane of symmetry was considered. Isothermal boundary condition was applied on bottom surface of micro channel in four different ways as given below (Fig. 3.2).

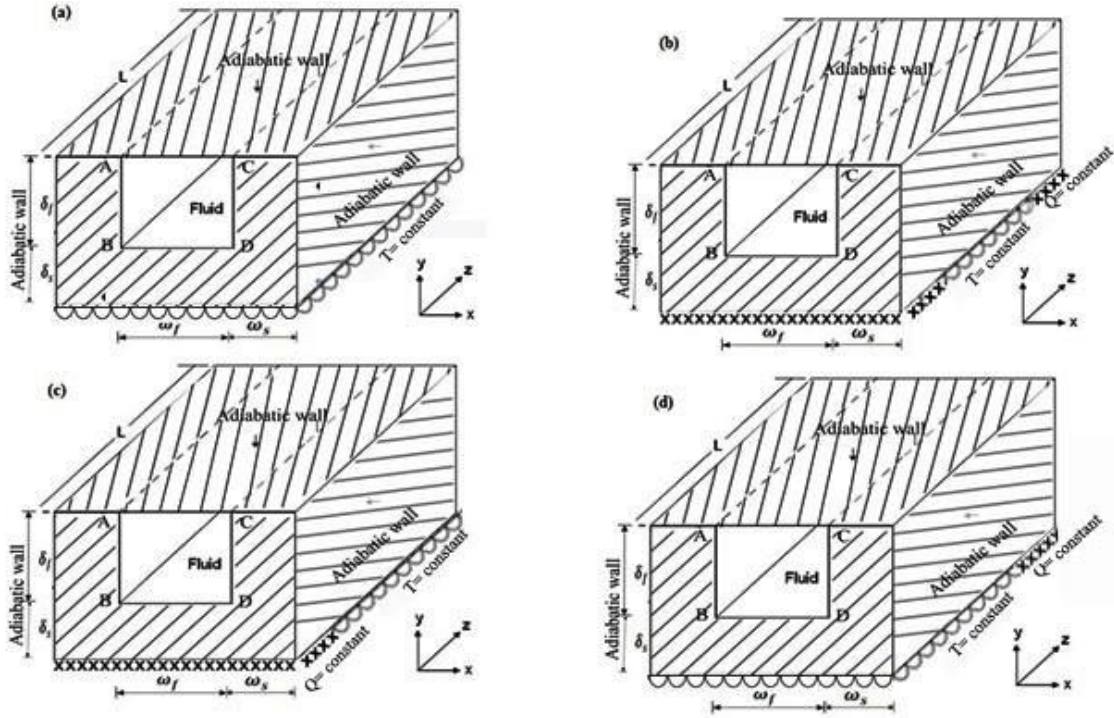


Fig. 3.2: Four different cases of heating the microchannel on its bottom face with constant wall temperature condition while keeping all other faces insulated (a) Heating over full length of microchannel substrate base (b) 6 mm insulated near inlet and outlet of bottom wall of the substrate (c) 6 mm insulated near inlet of bottom wall of the substrate (d) 6 mm insulated near outlet of bottom wall of the substrate.

Case 1: The entire bottom surface of microchannel is subjected to isothermal boundary condition while keeping all other outer surfaces insulated (Fig. 3.2 (a)).

Case 2: 6 mm of bottom surface is insulated from both inlet and outlet end of micro channel and remaining length (48 mm) of bottom surface is subjected to isothermal boundary condition (Fig. 3.2 (b)).

Case 3: 6 mm of bottom surface is insulated from inlet end of micro channel and remaining length (54 mm) of bottom surface is subjected to isothermal boundary condition (Fig. 3.2 (c)).

Case 4: 6 mm of bottom surface is insulated from outlet end of micro channel and remaining length (54 mm) of bottom surface is subjected to isothermal boundary condition (Fig. 3.2 (d)).

The governing equations are

For fluid domain:

$$\nabla \cdot \bar{u} = 0 \quad (3.1)$$

$$u \cdot \nabla \bar{u} = -\frac{1}{\rho} \nabla p + \frac{\mu}{\rho} \nabla^2 T \quad (3.2)$$

$$\bar{u} \cdot \nabla T = \left(\frac{k}{\rho} c_p \right) \cdot \nabla^2 T \quad (3.3)$$

For solid domain:

$$\nabla^2 T = 0 \quad (3.4)$$

The applicable boundary conditions are

$$\left(\frac{\partial T}{\partial x} \right) = 0, \text{ Y-Z plane at } x = 0 \text{ and } x = (2\omega_s + \omega_f) \quad (3.5)$$

$$\left(\frac{\partial T}{\partial y} \right) = 0, \text{ X-Z plane at } y = (\delta_s + \delta_f) \quad (3.6)$$

$$\left(\frac{\partial T}{\partial z} \right) = 0, \text{ X-Y plane at } z = 0 \text{ and } z = L \quad (3.7)$$

$$u = \bar{u}, \text{ X-Y plane at } z = 0 \quad (3.8)$$

$$u = 0, \text{ slip is absent at solid-fluid interfaces} \quad (3.9)$$

$$T = \text{Constant (350K)}, \text{ X-Z plane at } y = 0 \quad (3.10)$$

$$\text{Gauge pressure at } z = L \text{ and } y = 0 \text{ \& } y = \delta_s + \delta_f \quad (3.11)$$

$$\text{Partial heating or partial insulation at } z = 0 \text{ to } L \text{ and } y = 0 \quad (3.12)$$

The commercially available Ansys-Fluent[®] is used to solve the governing equation. For discretizing pressure term, Standard scheme is used and to solve governing equation ‘second order upwind’ method is used. The Simpler algorithm of Patankar [28] is used to resolve velocity-pressure coupling and in this study solution is deemed convergent when imbalance in momentum and energy equations is less than 10^{-6} and 10^{-9} respectively. Fluid is assumed to have a slug velocity profile at inlet and meshing was done using rectangular elements. To choose the best mesh size for study, a grid independence test is done.

3.2 Grid independence test

Grid independence test is carried out for a square channel with zero thickness as presented in Fig. 3.3 to choose the grid size. Using rectangular elements the entire computational domain is meshed and then sensitivity of grid is checked to choose the best mesh size. Local Nu_z is obtained for three different grids of $10 \times 20 \times 600$, $12 \times 24 \times 720$ and $14 \times 28 \times 960$. The intermediate mesh size is chosen since no appreciable change was noticed on further refinement of grid from $12 \times 24 \times 720$ to $14 \times 28 \times 960$. From Fig. 3.3, it can be observed that local Nu_z for intermediate mesh size ($12 \times 24 \times 720$) in fully developed region is close to theoretical Nu_z (equals 2.98) [29] observed for a fully developed flow in a square pipe subject to constant wall temperature boundary condition at its outer surface.

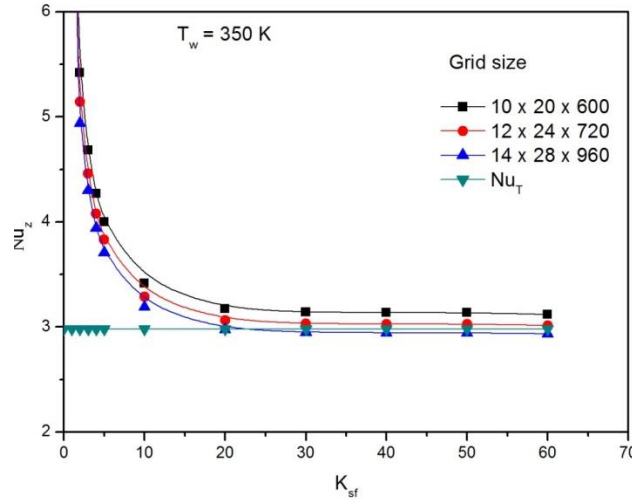


Fig. 3.3: Axial variation of local Nusselt number for $\delta_s = 0$ for three different mesh sizes.

3.3 Data reduction

For post processing of data following non dimensional variables are used. The non-dimensional axial coordinate is given by

$$z^* = \frac{z}{\text{Re } pr D_h} \quad (3.13)$$

The dimensionless local heat flux experienced at solid-fluid interface is given by

$$\phi = \frac{q_z}{q^*} \quad (3.14)$$

where q_z is heat at any location z calculated by peripheral average of heat flux along three conjugate walls and q^* is ratio of heat flux acting at substrates bottom and conjugate walls area.

$$q^* = \frac{q}{(\omega_f + \delta_f)} (2\omega_s + \omega_f) \quad (3.15)$$

The non- dimensional bulk fluid and inner wall temperature are given by

$$\theta = \frac{T - T_i}{T_o - T_i} \quad (3.16)$$

$$\theta_f = \frac{T_{f|z} - T_{fi}}{T_{fo} - T_{fi}} \quad (3.17)$$

$$\theta_w = \frac{T_{w|z} - T_{fi}}{T_{fo} - T_{fi}} \quad (3.18)$$

where T_i and T_o are fluid temperature at inlet and outlet respectively. The local Nusselt number is given by

$$Nu_z = \frac{h_z D}{k_f} \quad (3.19)$$

where local heat transfer coefficient is given by

$$h_z = \frac{q_z}{(T_w - T_f)} \quad (3.20)$$

The average Nu number over the channel length is given by

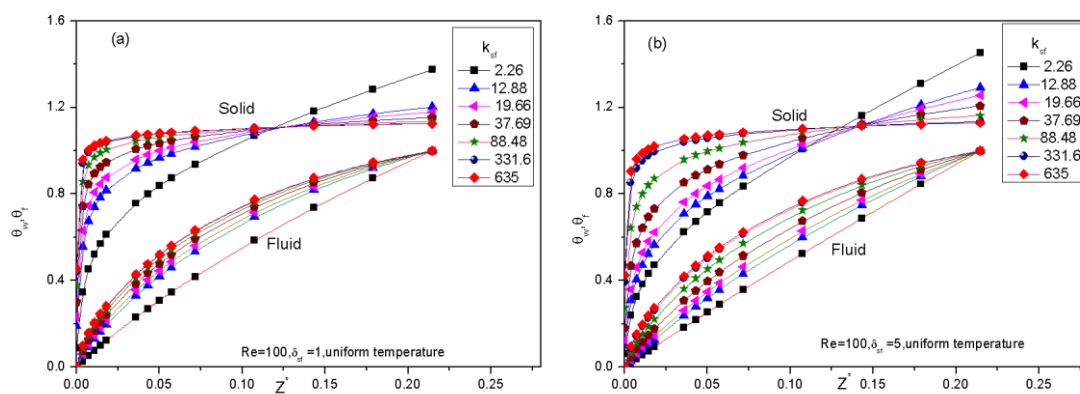
$$Nu_{avg} = \int_0^L Nu_z dz \quad (3.21)$$

Chapter 4

Results and discussion

As stated in chapter 3, keeping the width of substrate constant, the substrate thickness, Re , and substrate material are changed in different combinations to study the role of axial wall conduction on the conjugate heat transfer behaviour of a microchannel. Here it is to mention that for the square channel shown in Fig. 3.1(a) only the wall BD is parallel to bottom of substrate while the other two walls AB and DC are perpendicular to substrate bottom. Under ideal condition (zero wall thickness), value of Nusselt number is 2.98 [29] for constant thermal boundary conditions applied on surface of a rectangular duct. Since boundary condition is applied away from liquid-wall interface effective heat transfer coefficient is likely to be different from that predicted for a channel with zero thickness. The aim of this study is to determine the actual boundary condition experienced at the solid-fluid interface of a square micro channel subjected to partial heating by constant wall temperature applied at its bottom surface and its effect on heat transfer behaviour of micro channel. The parameters that will determine the extent of axial conduction in substrate are axial variation of average bulk fluid temperature, average heat flux and average channel wall temperature.

First, the bottom surface of microchannel is heated over its entire length such that constant temperature is maintained over the full length of microchannels substrate base while the remaining surfaces are kept insulated.



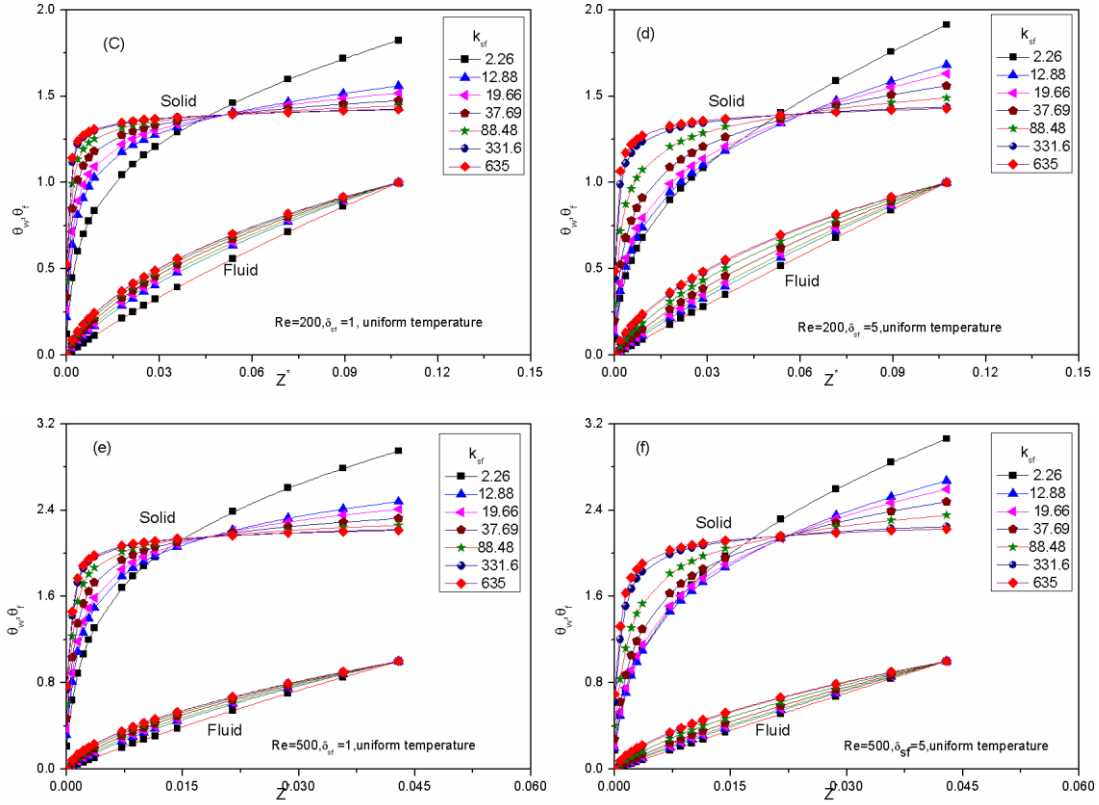


Fig. 4.1: Axial variation of dimensionless wall temperature and fluid temperature as function of δ_{sf} , k_{sf} and Re (for heating as per Case-1).

It can be observed in Fig. 4.1 that at lower Reynolds number ($Re = 100$), lower value of δ_{sf} (equal 0.5) and for larger k_{sf} value fluid temperature is varying parabolically which is the case when channel is subjected to isothermal boundary conditions (see Fig 1.1.(b)). Also except near the inlet area the wall temperature is almost constant throughout the microchannel. From these observations, it can be concluded that for this case there is no axial heat conduction.

Now as the value of δ_{sf} is increased while keeping all other parameters constant, the fluid temperature varies linearly suggesting that constant temperature boundary condition is compromised by axial conduction. In other words, the axial conduction causes the actual condition experienced at fluid-solid boundary interface to drift more towards iso-flux boundary conditions although isothermal boundary conditions was applied at bottom of the substrate. It can be also observed that the gap between wall and fluid temperature remains constant once flow is fully developed especially for lower k_{sf} values.

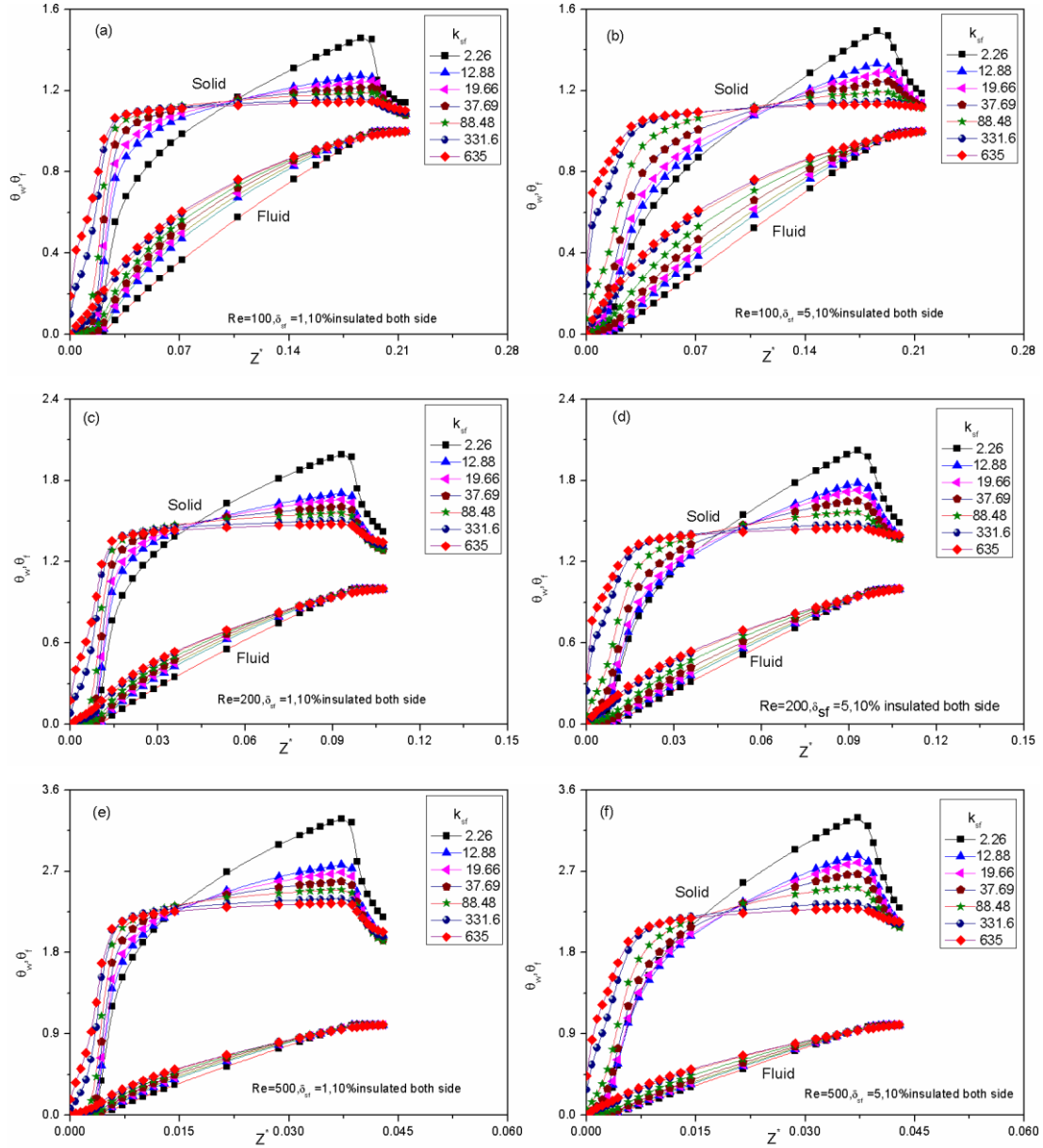


Fig. 4.2: Axial variation of dimensionless wall temperature and fluid temperature as function of δ_{sf} , k_{sf} and Re (for heating as per Case-2).

Fig. 4.2 shows the plot corresponding to Fig. 4.1, for case-2. i.e. 6 mm length each of bottom face is insulated from both inlet and outlet end and the remaining length of bottom face are subjected to uniform heating while all other surfaces are kept insulated. Under ideal condition bulk fluid temperature and the wall temperature in the insulated region should be same as the inlet fluid temperature but in reality that's not the case. Due to finite conductivity of material, there will be an axial conduction near the inlet in a direction opposite to flow direction. The axial conduction causes a rise in both fluid and wall temperature in the 6 mm insulated region near the inlet and this rise in temperature becomes

more visible with increasing k_{sf} values because of the lower resistance offered to heat flow by conduction (see Fig. 4.2 (a)).

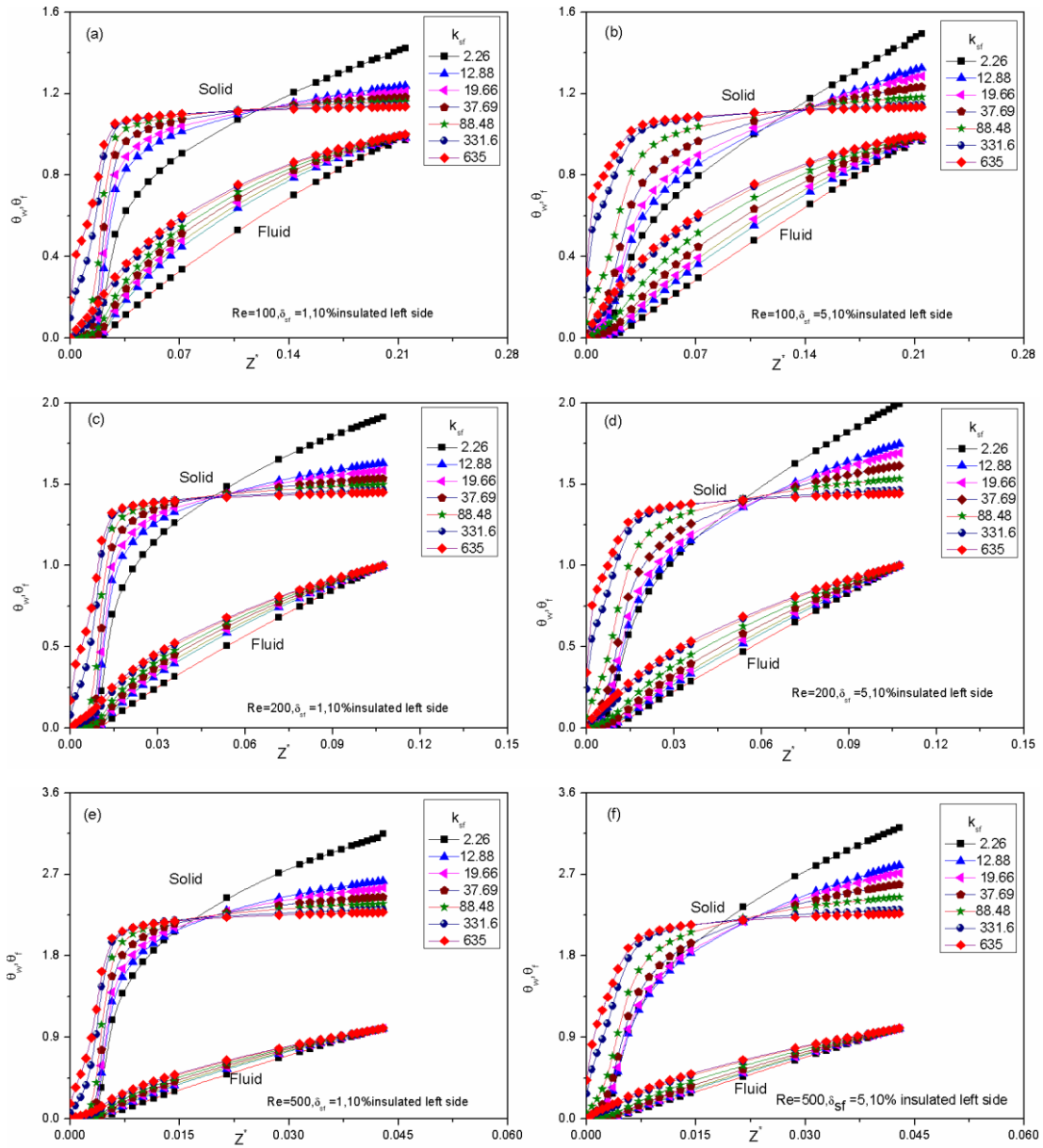


Fig. 4.3: Axial variation of dimensionless wall temperature and fluid temperature as function of δ_{sf} , k_{sf} and Re (for heating as per Case-3).

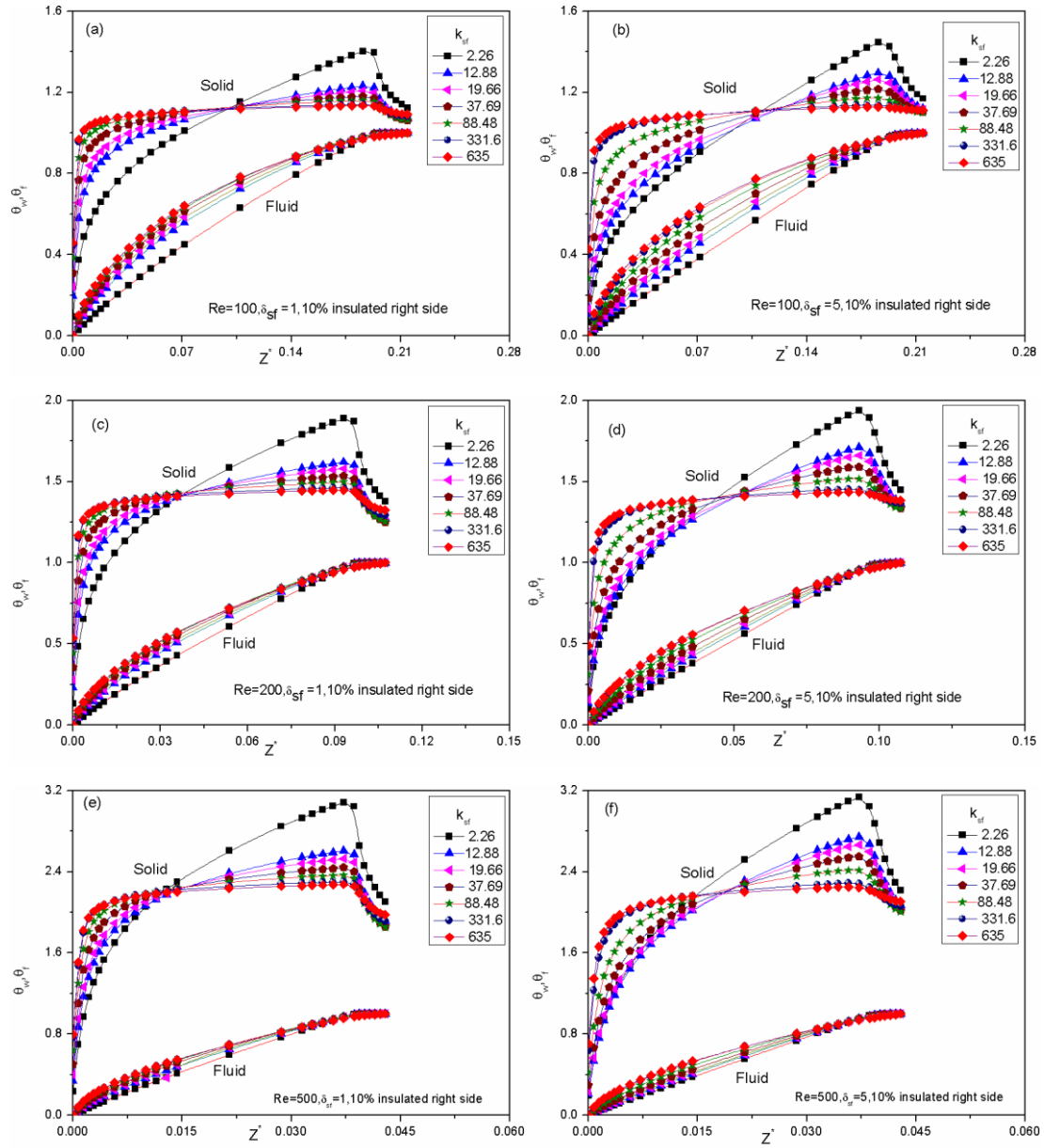


Fig. 4.4: Axial variation of dimensionless wall temperature and fluid temperature as function of δ_{sf} , k_{sf} and Re (for heating as per Case-4).

Under same condition, higher the cross sectional area of solid lower is the resistance to axial conduction. This can be understood by just comparing slopes of wall temperature in 6 mm insulated region near the inlet of Fig. 4.2 (a) and 4.2 (b). It is evident from Fig. 4.2 (b) that slope of wall temperature in 6 mm insulated region near the inlet is higher than its counterpart in Fig. 4.2 (a). It can be also observed that as value of Reynolds number increases, fluid temperature begins to drift from parabolic to linear variation indicating that for higher Reynolds number, the boundary condition at the interface moves more towards constant wall heat flux condition.

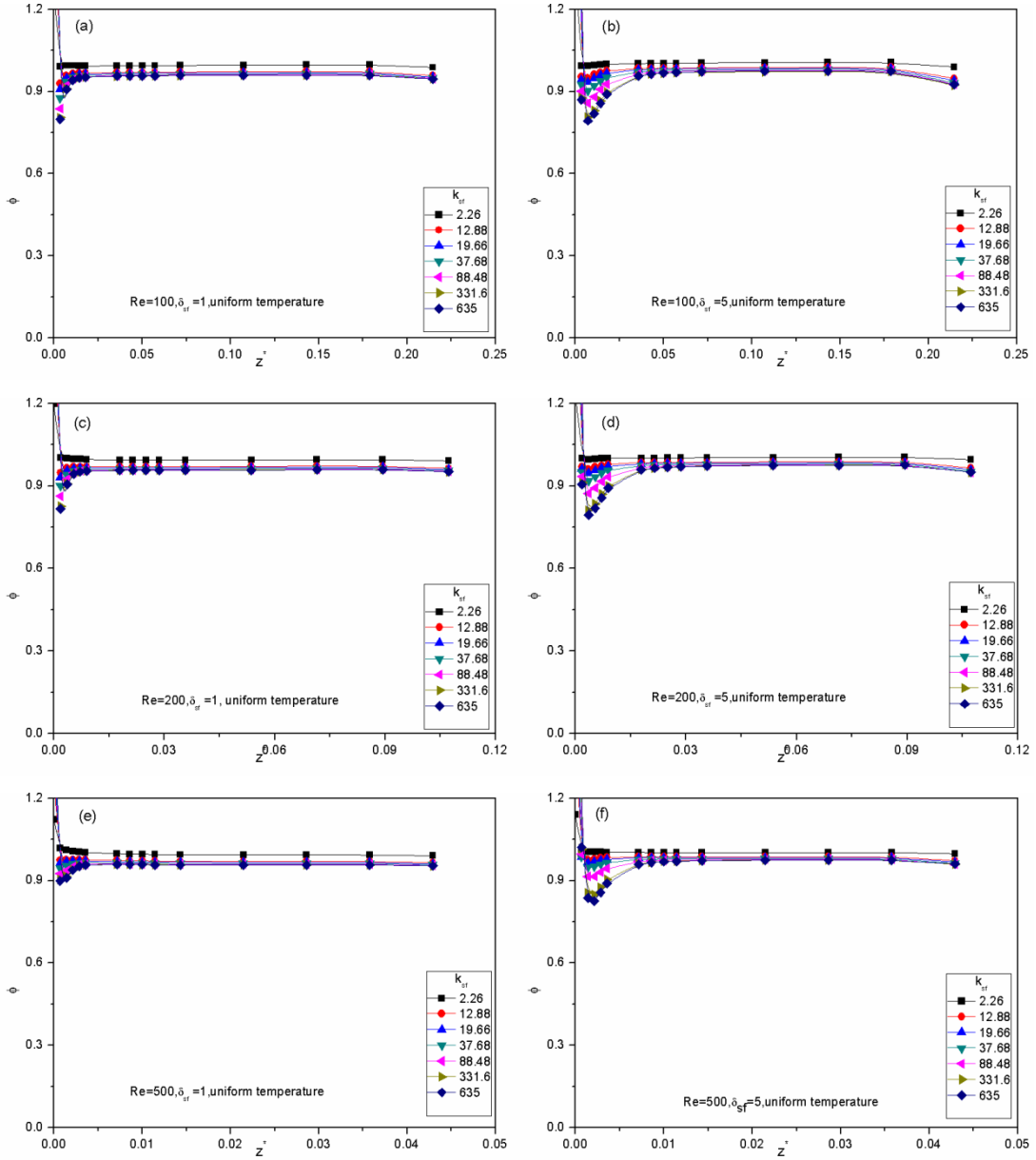


Fig. 4.5: Axial variation of dimensionless local heat flux as function of δ_{sf} , k_{sf} and Re (for heating as per Case-1).

It can be observed from Fig. 4.2 (a) that for 6 mm insulated region near the outlet, the fluid temperature remains almost same for case of $\delta_{sf} = 1$ because no heat is added in this region. Also since the wall temperature is only slightly higher than fluid temperature there will be no heat transfer from wall to fluid, except at lower k_{sf} . For lower k_{sf} value, wall temperature will begin to decrease in the 6 mm insulated region near the outlet in the flow direction because of heat transfer from wall to fluid. It can be also seen by comparing Fig. 4.2 (e) and Fig. 4.2 (a) that fluid temperature differ wall temperature by a higher value for higher flow Re in the 6 mm insulated region near the outlet. Thus for higher Re, wall temperature

will begin to decrease in the direction of flow of fluid because of heat transfer from wall to fluid.

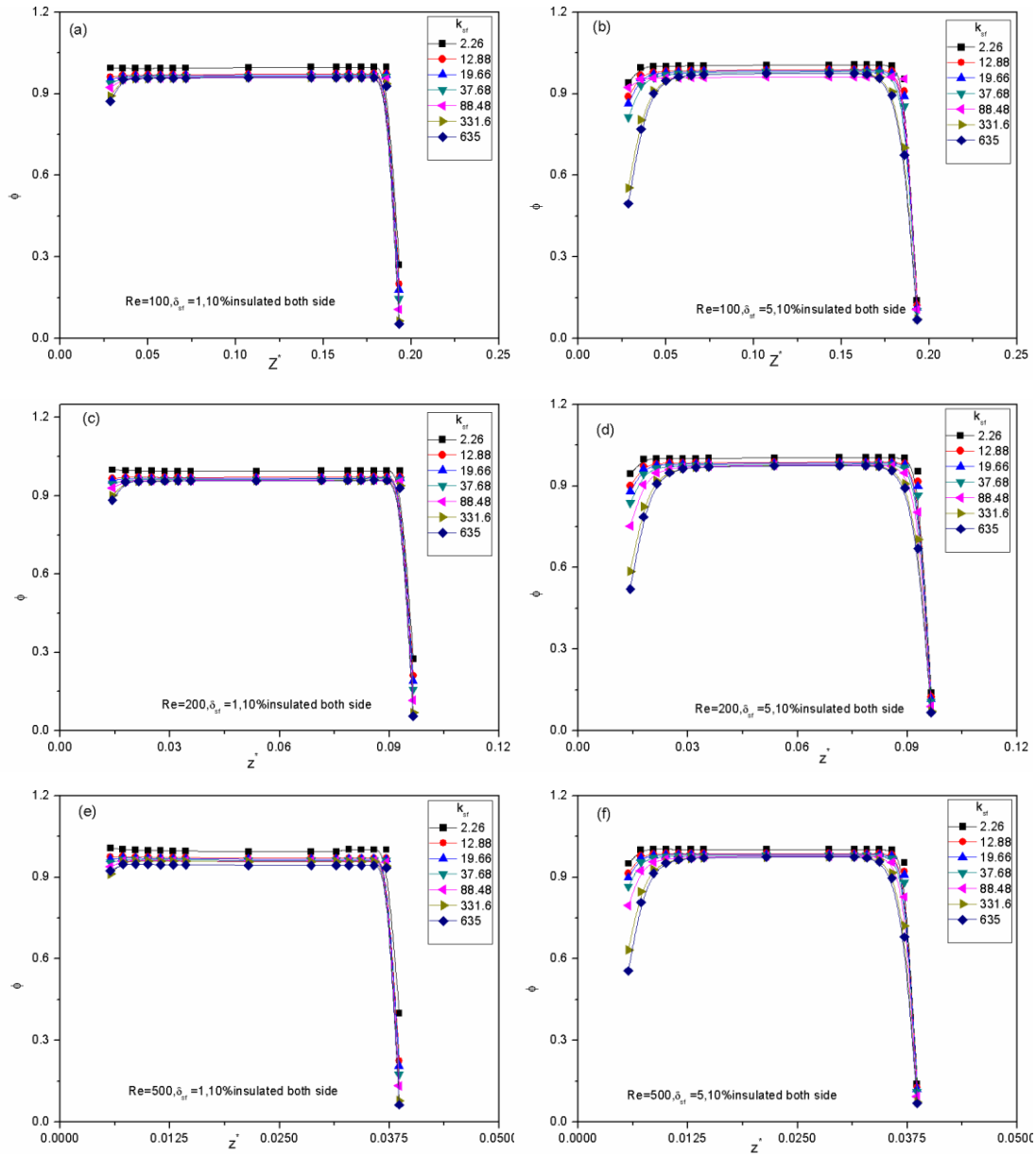


Fig. 4.6: Axial variation of dimensionless local heat flux as function of δ_{sf} , k_{sf} and Re (for heating as per Case-2).

Fig. 4.3 shows the plot corresponding for case-3 i.e. 6 mm length of bottom face is insulated from inlet end and the remaining bottom face is subjected to constant wall temperature boundary condition while all other surfaces are kept insulated. Geometrically this is similar to Case-2 heating the difference being here 6 mm length from outlet side is also subjected to constant wall temperature. Thus variation in parameters in Fig. 4.3 are almost similar to portion of curve to left of 6 mm insulated region from outlet end in Fig. 4.2.

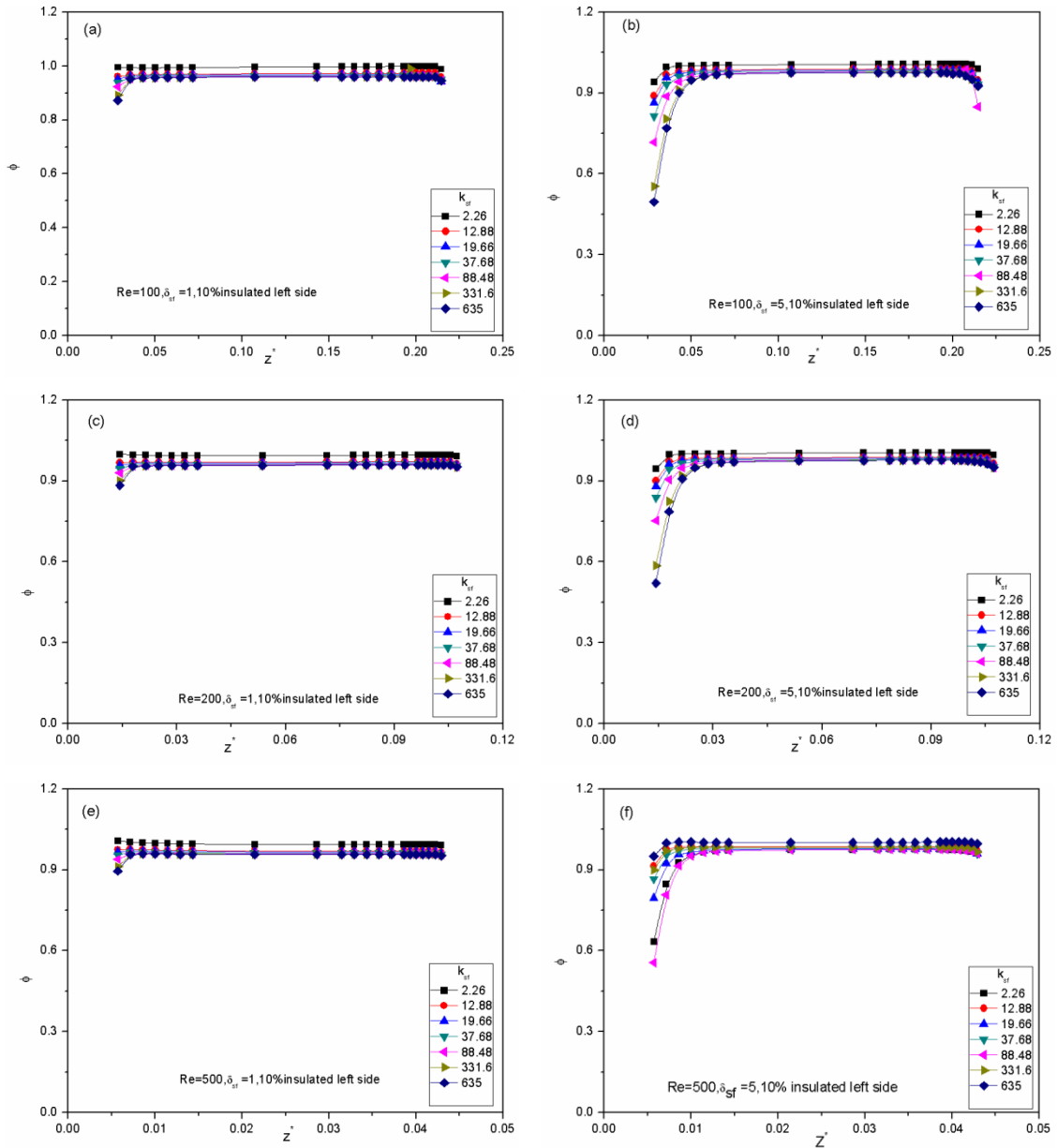


Fig. 4.7: Axial variation of dimensionless local heat flux as function of δ_{sf} , k_{sf} and Re (for heating as per Case-3).

Geometrically this is similar to Case-2 heating the difference being here 6 mm length from inlet side is also subjected to constant wall temperature. Thus variation in parameters in Fig. 4.4 are almost similar to portion of curve to right of 6 mm insulated region from inlet end in Fig. 4.2. The axial variation of dimensionless heat flux is presented in Fig. 4.5 to understand the heat flux actually experienced at the interface of solid and fluid.

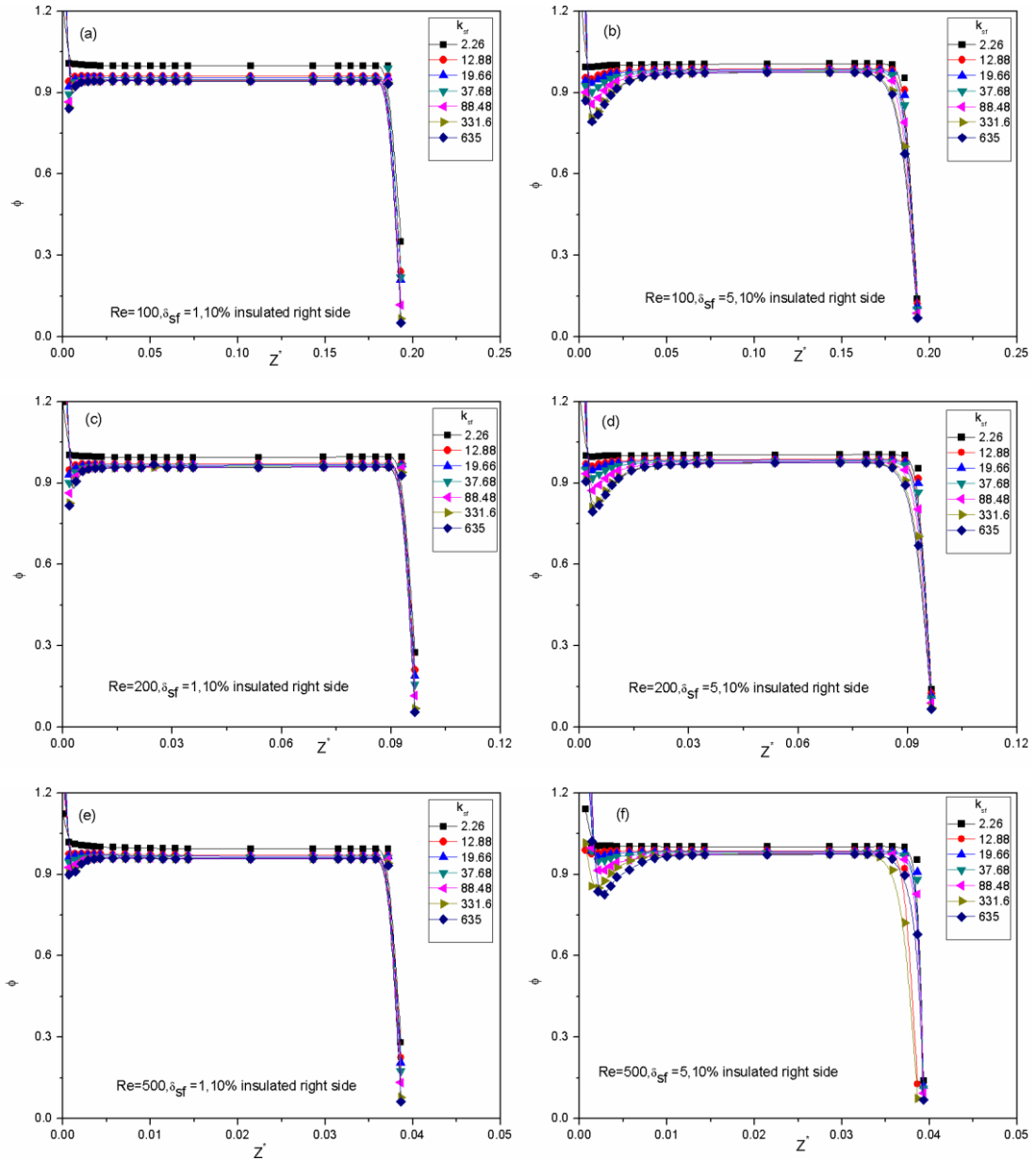


Fig. 4.8: Axial variation of dimensionless local heat flux as function of δ_{sf} , k_{sf} and Re (for heating as per Case-4).

It can be seen that heat flux experienced for lower k_{sf} at solid-fluid interface is axially constant but for higher k_{sf} heat flux experienced at interface is found to deviate from theoretical value with increasing δ_{sf} . This behaviour can be attributed to axial conduction phenomenon. At higher k_{sf} , material will offer less resistance to conduction leading to significant axial conduction resulting in a considerable drop in amount of heat flux transfer taking place from solid to fluid. It can be seen from Fig. 4.5 (a), Fig. 4.5 (b), Fig. 4.5 (c) and Fig. 4.5 (d) that heat flux experienced at the solid-fluid interface is mainly dependent

on the wall thickness when constant temperature is applied in different combinations on the bottom substrate of microchannel.

Zhang et al. [17] has reported a similar observation that dimensionless heat flux at solid-fluid interface of a circular pipe subjected to isothermal boundary condition at its outer surface tends to become constant once axial conduction becomes substantial.

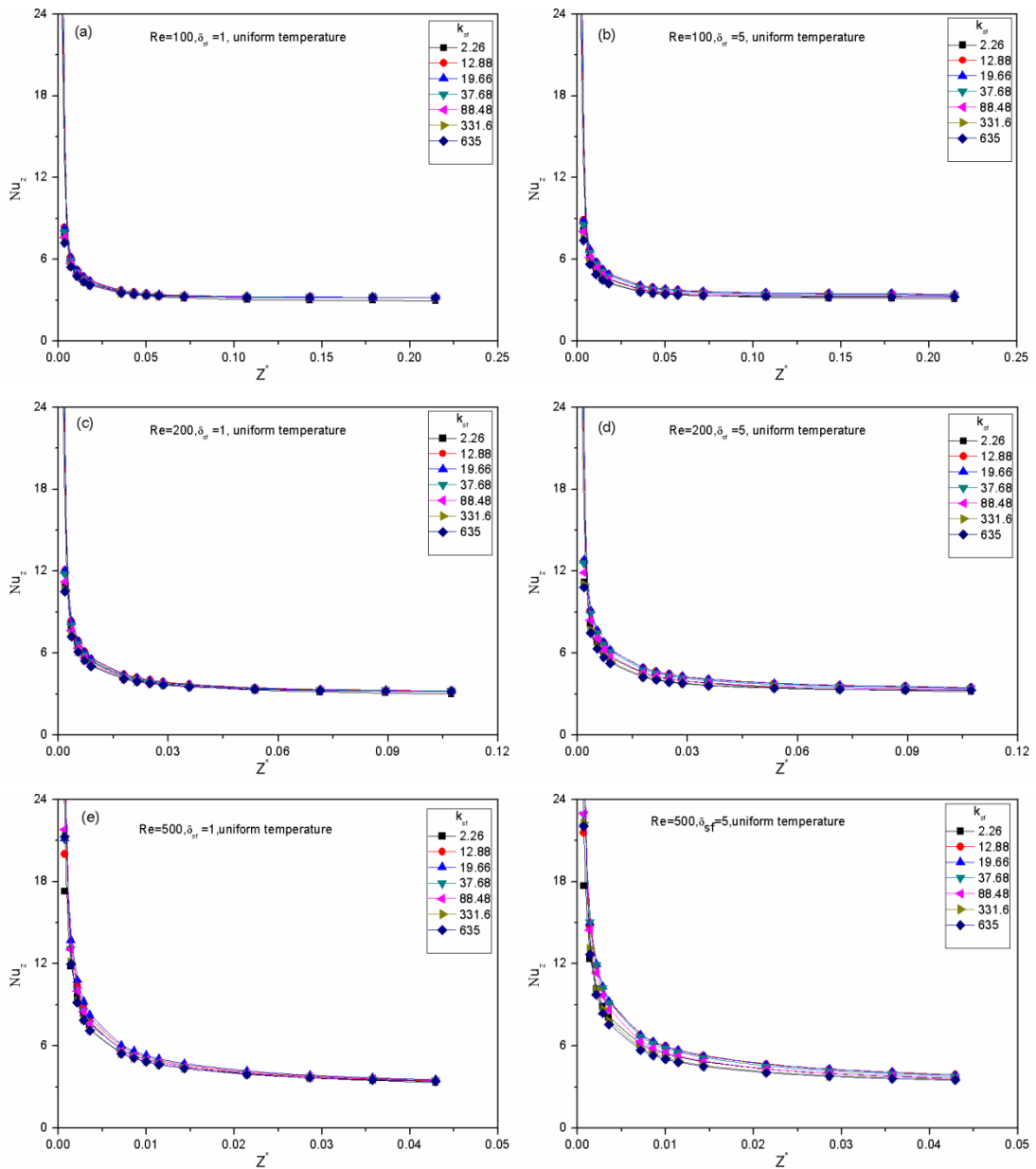


Fig. 4.9: Axial variation of local Nusselt number as function of δ_{sf} , k_{sf} and Re (for heating as per Case-1).

By observing the above given figures representing axial variation of dimensionless heat flux for different cases it can be concluded that heat flux is a strong function of thickness

ratio (δ_{sf}) and both Re and k_{sf} have minimum effect on dimensionless heat flux because of axial back conduction.

Fig. 4.9 to Fig. 4.12 represents the axial variation of local Nusselt number observed in the different cases.

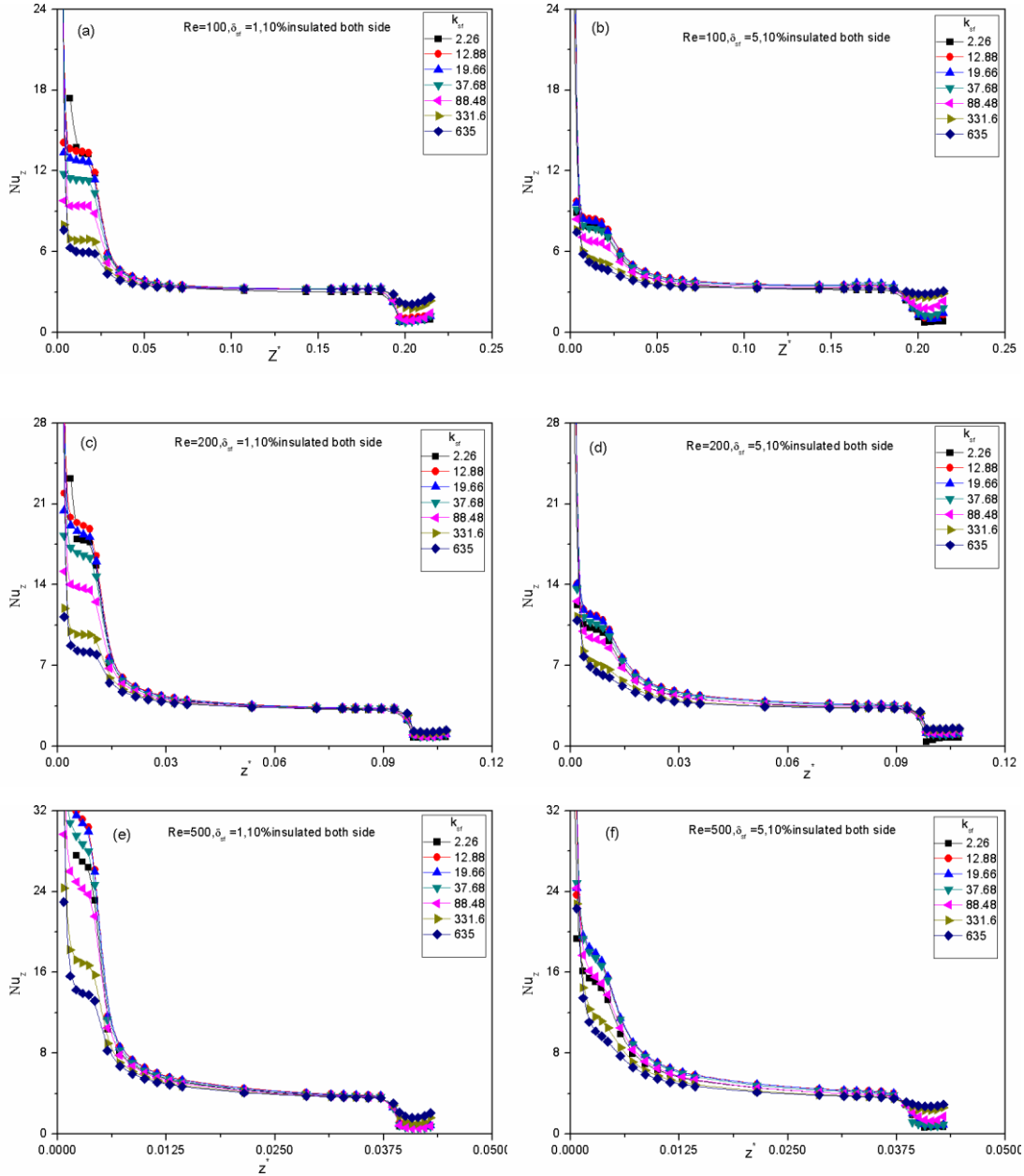


Fig. 4.10: Axial variation of local Nusselt number as function of δ_{sf} , k_{sf} and Re (for heating as per Case-2).

The Nu_z for low flow Re and lower wall thickness can be observed to increase with decrease in value of k_{sf} (see Fig. 4.9 (a)). It can be observed from Fig. 4.9 (b) that, as δ_{sf} is increased keeping all other parameters same, the value of Nu at any axial location increases

for any k_{sf} because of the axial conduction. This increase in δ_{sf} is however sensitive to variation in k_{sf} , and it can be seen that lower the k_{sf} higher is the increase in Nu value.

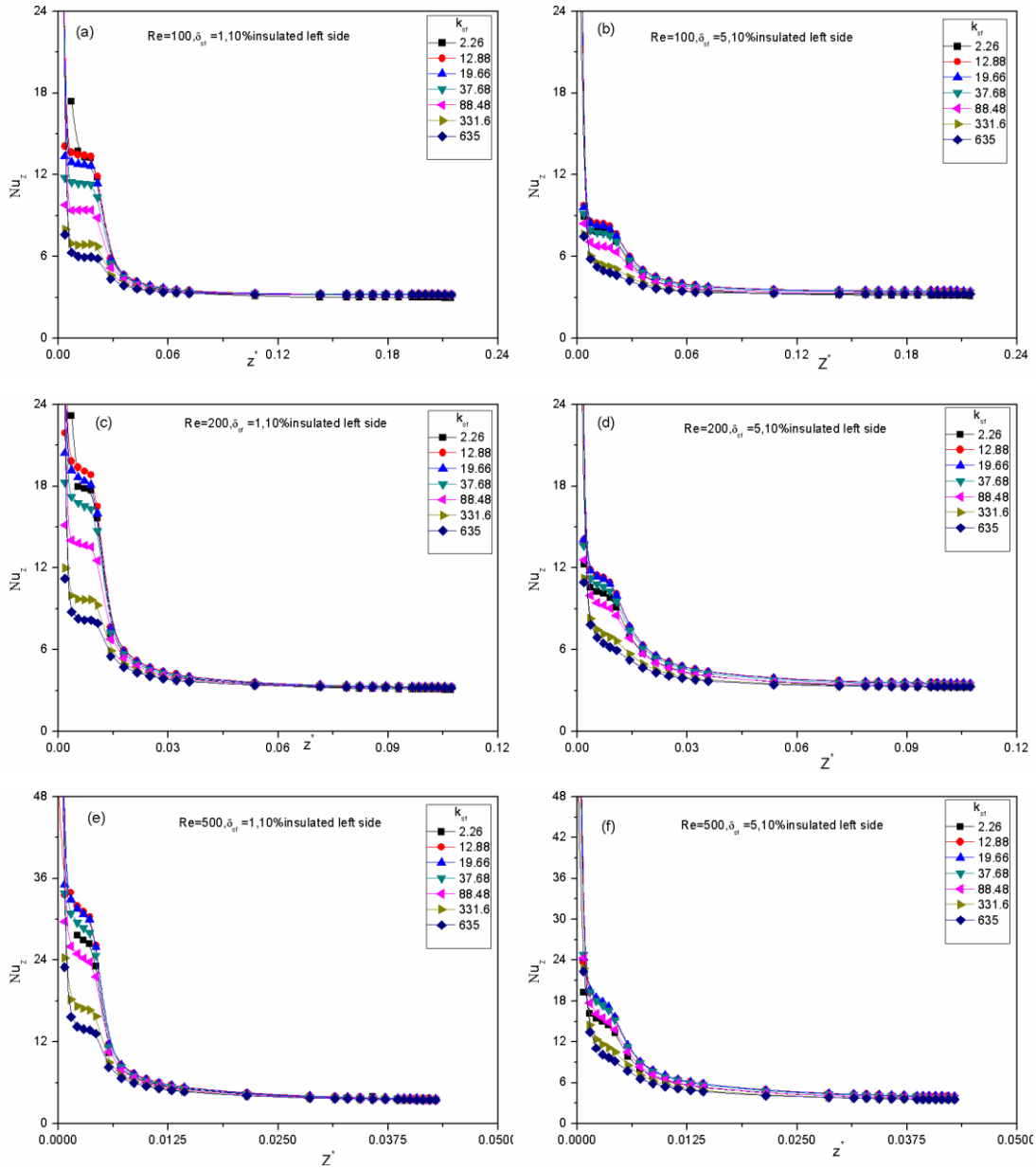


Fig. 4.11: Axial variation of local Nusselt number as function of δ_{sf} , k_{sf} and Re (for heating as per Case-3).

It can be observed that local Nu remains same at the inlet end up to insulated region (6 mm from inlet end) and then it decreases suddenly to fully developed flow and again it decreases suddenly at the outlet (6 mm from outlet end) and later increases in insulated region. For a wide range of k_{sf} , Re and δ_{sf} axial variations of local Nusselt number are represented in the Fig. 4.9-4.12.

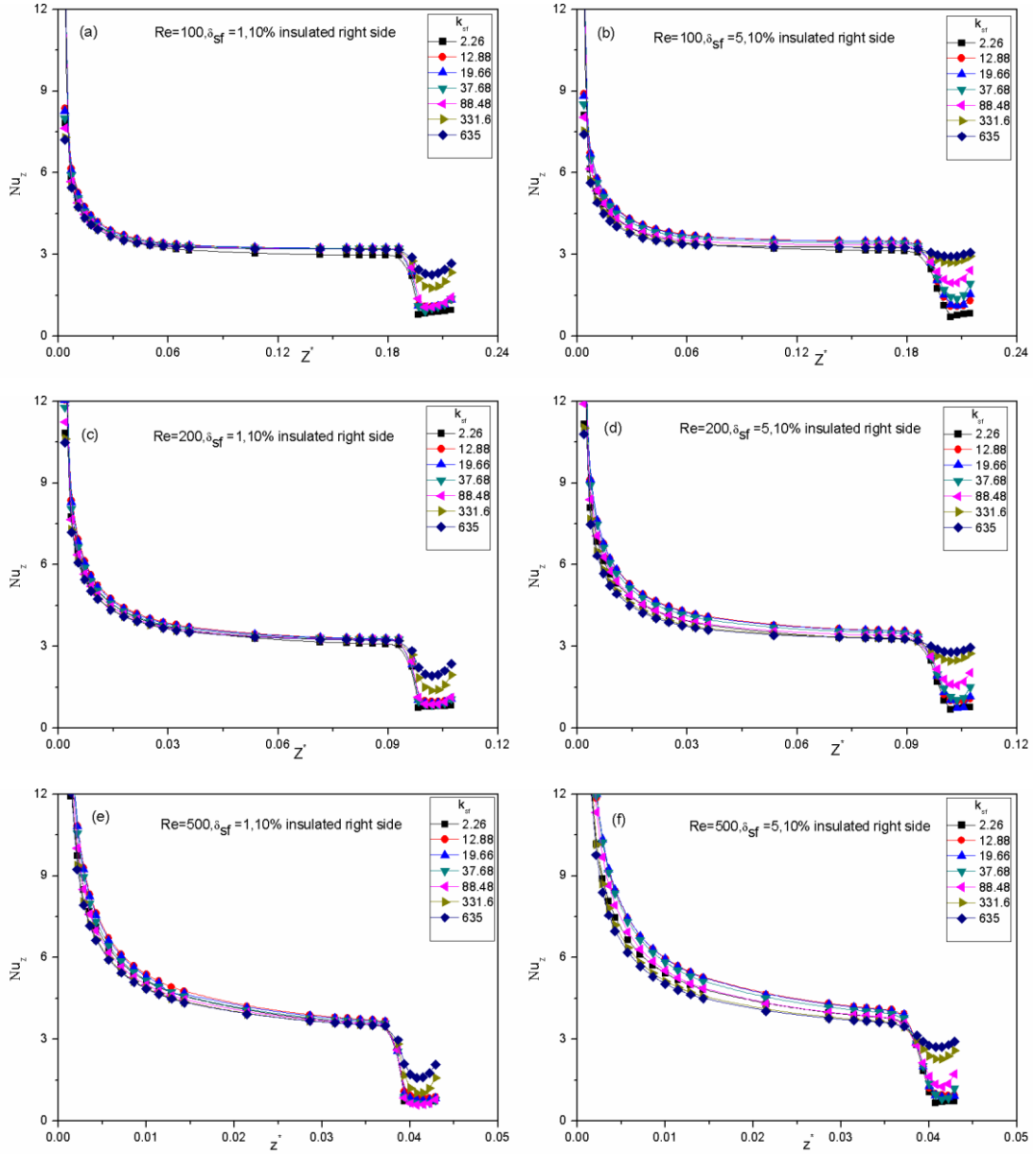


Fig. 4.12: Axial variation of local Nusselt number as function of δ_{sf} , k_{sf} and Re (for heating as per Case-4).

As explained earlier Case-3 and Case-4 heating are geometrically similar to Case-2 heating the difference being 6 mm length from outlet side is also subjected to constant wall temperature in the first case (i.e. Case-2) and 6 mm length from inlet side is also subjected to constant wall temperature in latter case (i.e. Case-3) respectively. Thus deviations observed in parameters for Case-3 and Case-4 (see Fig. 4.11 and Fig. 4.12) are almost similar in nature to variation in parameters observed for Case-2 (see Fig. 4.9).

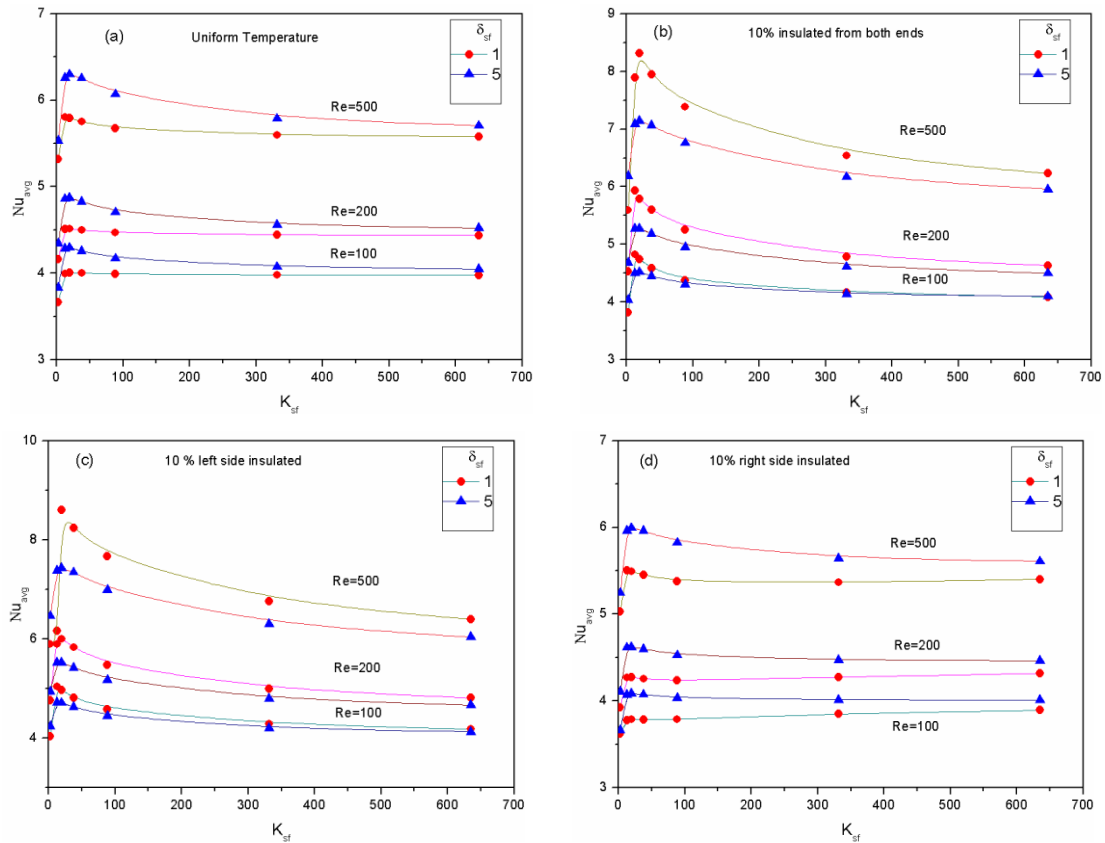
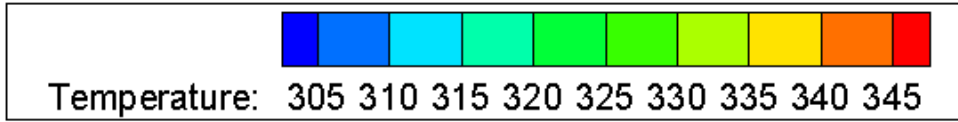


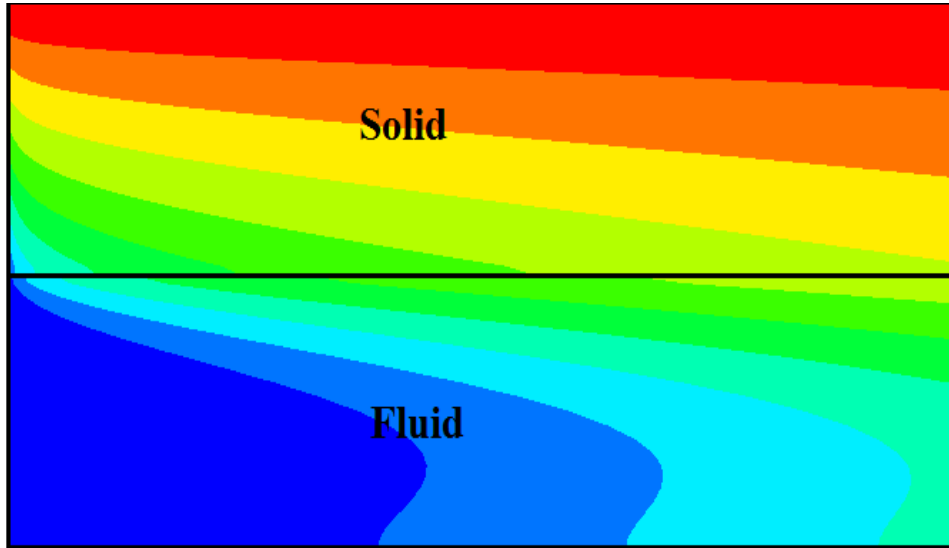
Fig. 4.13: Variation of average Nusselt number with k_{sf} for $Re = 100-500$ and $\delta_{sf} = 1-5$ for different cases of heating the microchannel (a) Heating over full length of microchannel substrate base (b) 6 mm insulated near inlet and outlet of bottom wall of the substrate (c) 6 mm insulated near inlet of bottom wall of the substrate (d) 6 mm insulated near outlet of bottom wall of the substrate.

For lower k_{sf} , through vertical faces (AB and CD) heat flux is less than the flux through horizontal face (BD) changing it into a one sided heating problem while for higher k_{sf} values axial conduction will come into play causing a drop in Nu_{avg} value.

It can be also noticed that as δ_{sf} increases, the axial variation of wall temperature at solid-fluid interface drifts more towards the constant heat flux trend due to axial back conduction. This causes higher Nusselt number for micro channels having thicker walls.



For $\delta_{sf} = 1$,



For $\delta_{sf} = 5$,

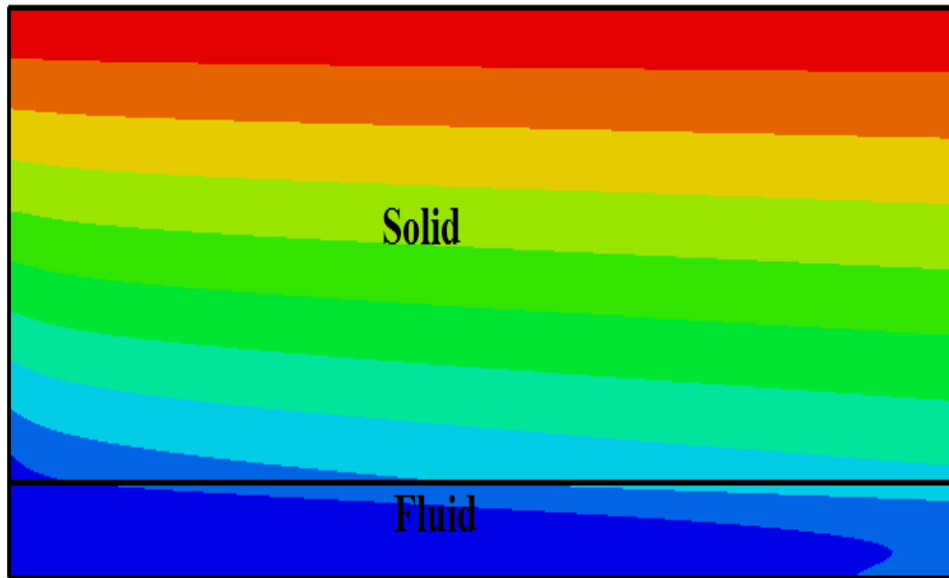
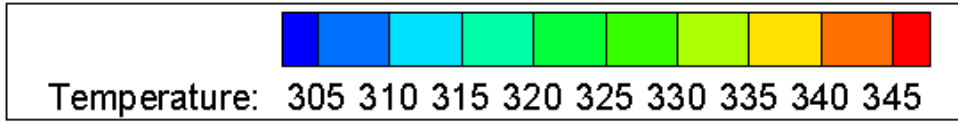
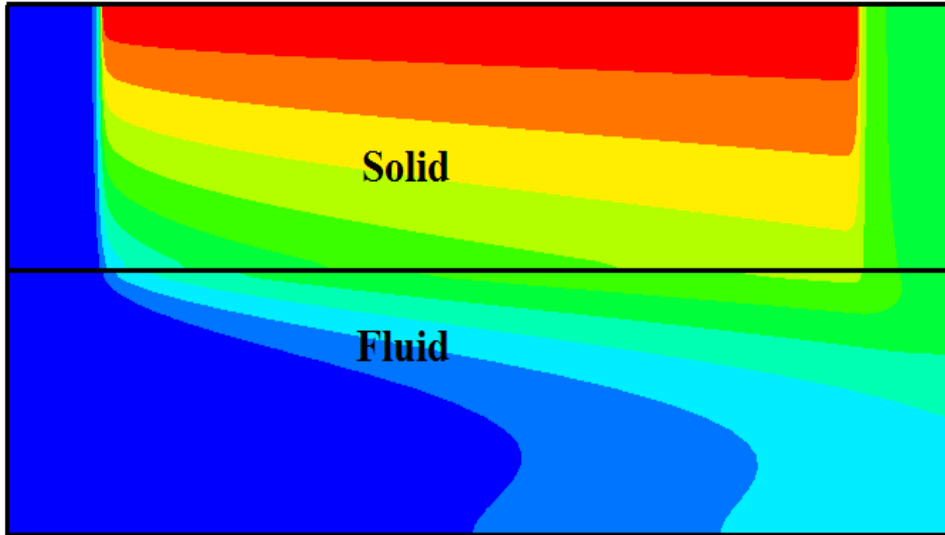


Fig. 4.14: Temperature contours for Case 1(Heating over full length of microchannel substrate base).



For $\delta_{sf} = 1$,



For $\delta_{sf} = 5$,

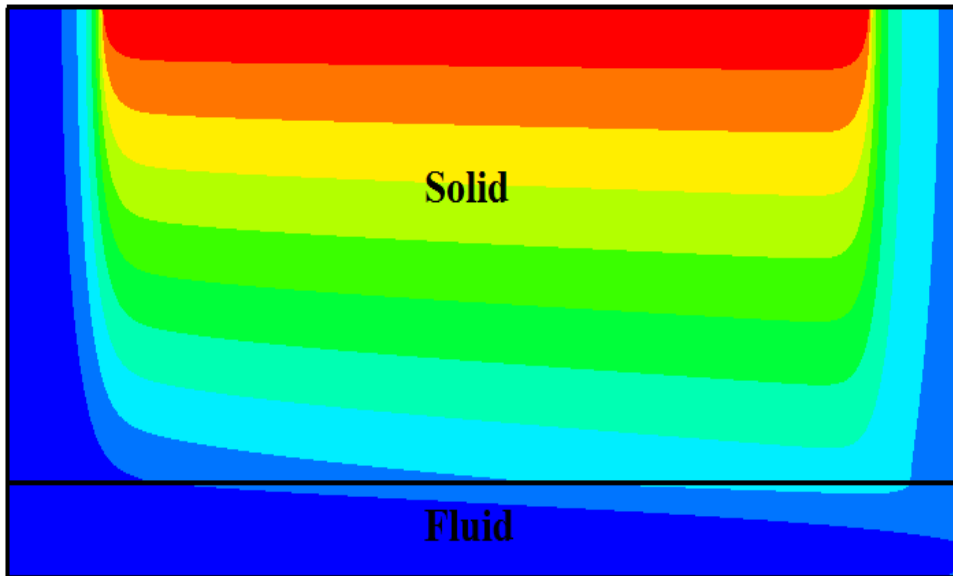
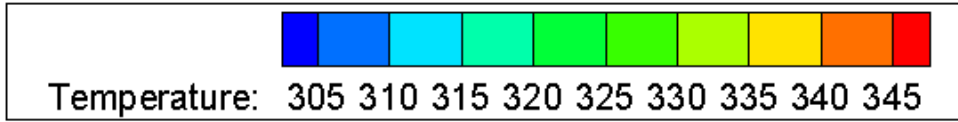
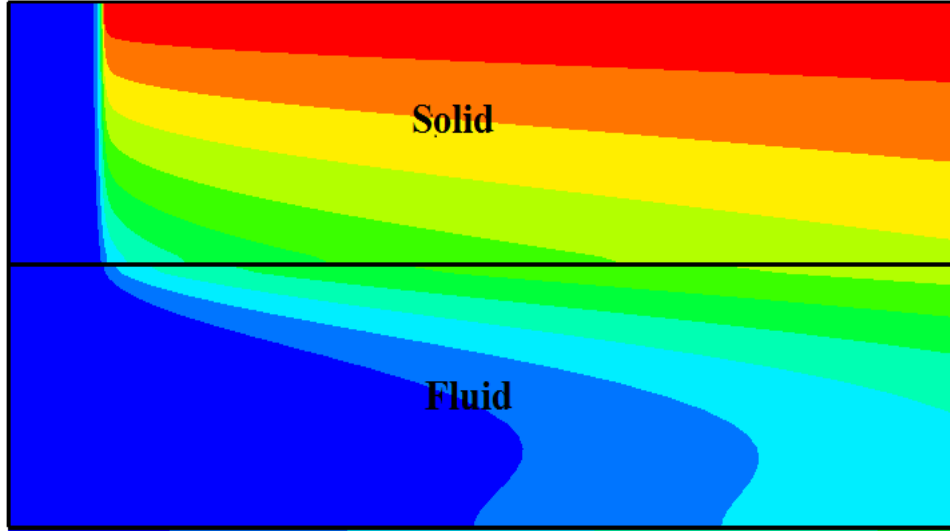


Fig. 4.15: Temperature contours for Case 2 (6 mm insulated near inlet and outlet of bottom wall of the substrate).



For $\delta_{sf} = 1$,



For $\delta_{sf} = 5$,

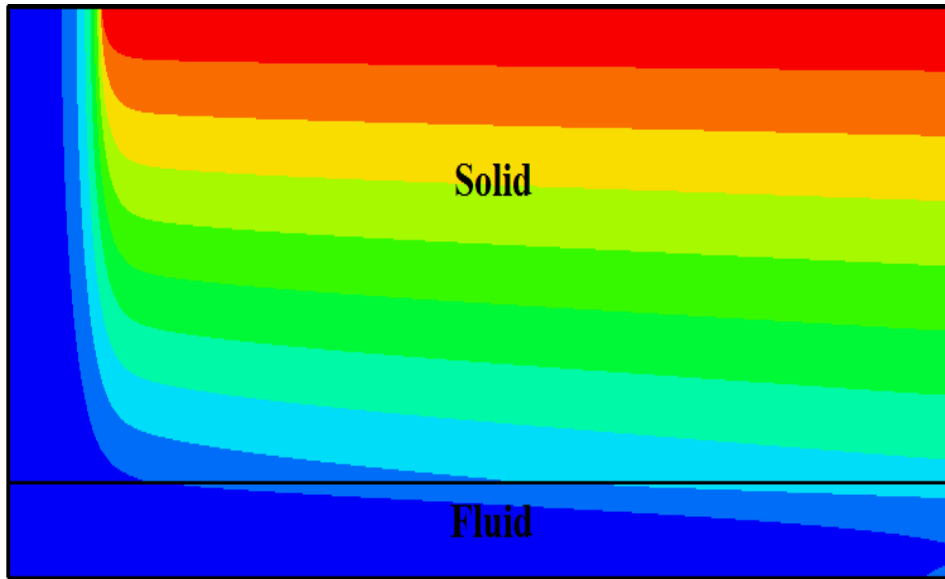
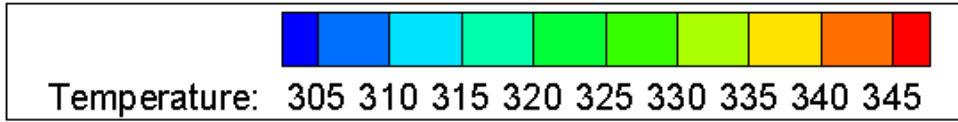
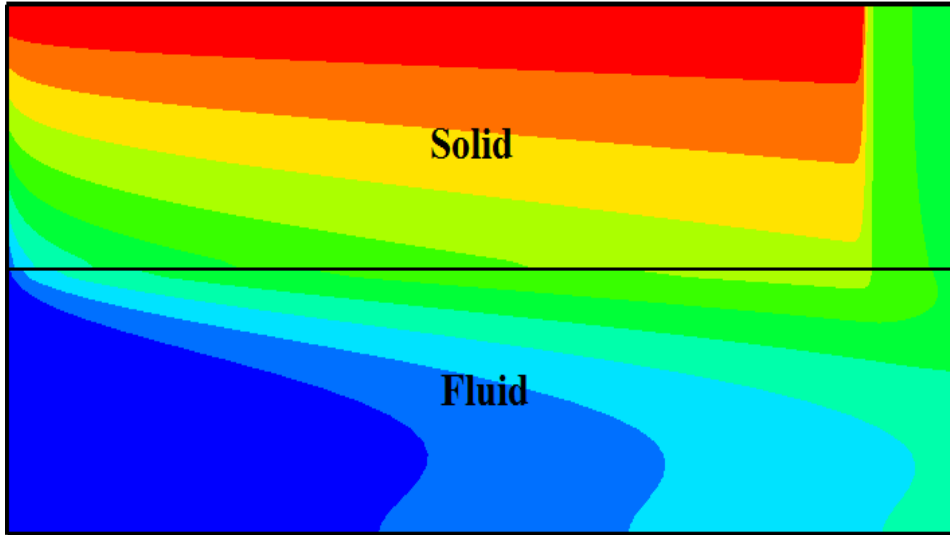


Fig. 4.16: Temperature contours for Case 3 (6 mm insulated near inlet of bottom wall of the substrate).



For $\delta_{sf} = 1$,



For $\delta_{sf} = 5$,

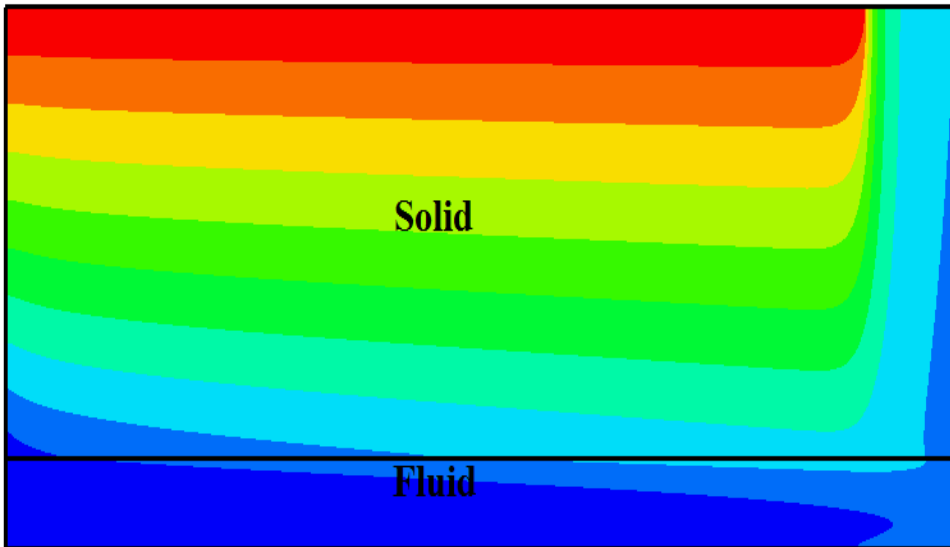


Fig. 4.17: Temperature contours for Case 4 (6 mm insulated near outlet of bottom wall of the substrate).

Chapter 5

Conclusion

A three-dimensional numerical study is carried out to understand the influence of axial wall conduction on the heat transfer in a rectangular micro channel subjected to isothermal boundary condition on its bottom face. Four different cases has been considered keeping practical application in mind: (i) Bottom surface of micro channel is heated over its entire length while all other surfaces are kept insulated (ii) 6 mm length each of bottom face is insulated from both inlet and outlet end and remaining length of bottom face is subjected to constant wall temperature boundary condition while all other surfaces are kept insulated (iii) 6 mm length of bottom face is insulated from inlet end and the remaining bottom face is subjected to constant wall temperature boundary condition while all other surfaces are kept insulated (iv) 6 mm length of bottom face is insulated from outlet end and remaining bottom face is subjected to constant wall temperature boundary condition while all other surfaces are kept insulated. Computations are carried out for wide range of parameters: conductivity ratio (k_{sf} : 2-635), thickness ratio (δ_{sf} : 1-5) and flow Re (100-500).

The main observations of this study are:

- ❖ For fully heated micro channel, it is found that value of Nu_{avg} is increasing with decreasing value of k_{sf} upto k_{sf} approximately equal to 25 and beyond that on decreasing k_{sf} value further, value of Nu_{avg} starts to decrease rapidly. This sudden decrease in Nu_{avg} value is because under such situation the case becomes a one sided heating problem rather than three sided heating problem. Now as k_{sf} is increased beyond a range, axial back conduction comes into play and this causes value of Nu_{avg} to decrease. Thus, for given flow Re and wall thickness ratio Nu_{avg} is maximum for an optimum k_{sf} . Difference between average Nu values at lower k_{sf} can be seen to be higher than that at higher k_{sf} values. Finally in comparison to higher δ_{sf} , for lower δ_{sf} Nu_{avg} has higher values due to axial back conduction.
- ❖ Trend similar to that seen in case of full heating is observed for remaining cases with some deviation as mentioned below. The difference between average Nu values at any k_{sf} is higher than corresponding average Nu value for full heating.

- ❖ For a given flow Re and δ_{sf} , k_{sf} plays the dominant role in determining the influence axial conduction on heat transport behaviour.
- ❖ Normally higher axial conduction causes solid fluid interface boundary conditions to drift more towards iso flux condition although isothermal condition is applied on outer surface.
- ❖ For a given k_{sf} , axial back conduction has minimum effect for low δ_{sf} , thus least possible thickness should be employed for increasing Nu in channel.
- ❖ It can be concluded that low conductive thin micro channels experiencing high flow rates has minimum effect of axial back conduction on heat transfer.
- ❖ Depending on the situation axial conduction may enhance or reduce heat transfer.

References:

1. Khandekar S., Moharana M.K., 2014, Some Applications of Micromachining in Thermal-Fluid Engineering, Chapter in: Introduction to Micromachining, 2nd Edition, Editor: Dr. V. K. Jain, Narosa Publishing House.
2. Tuckerman D.B., and Pease R.F., 1981, High-performance heat sinking for VLSI, IEEE Electron Device Letters, IEEE,2(5), pp. 126-129.
3. Incropera F.P., Dewitt D.P., Bergman L.T., and Lavine A.S., Fundamentals of Heat and Mass Transfer, John Wiley and Sons, 7ed, pp.531-532.
4. Hong C., Yamamoto T., Asako Y., and Suzuki K., 2011, Heat transfer characteristics of compressible laminar flow through microtubes, Journal of Heat Transfer, 134(1), 011602-01-08.
5. Philips R.J., 1988, Micro channel heat sinks, The Lincoln Laboratory Journal, 1(1), 31-48.
6. Peng X.F., and Peterson G.P, 1996, The effect of thermofluid and geometrical parameters on convection of liquid through rectangular micro channels, International Journal Heat Mass transfer, 38(4), pp. 681-689.
7. Adams T.M., Abdel-Khalik S.I., Jeter S.M., and Qureshi Z. H., 1998, An experimental investigation of single phase forced convection in micro channels, International Journal of Heat and Mass Transfer, 41(6), pp. 851-857.
8. Kim S.J. and Kim D., 1999, Forced convection in micro structures for electronic equipment cooling, Journal Heat transfer, 121(3), pp. 639-645.
9. Fedorov A.G and Viskana R., 2000, Three dimensional conjugate heat transfer in the micro channel for electronic packaging, International Journal of Heat and Mass Transfer, 43(3), pp. 399-415.
10. Ryu J.H., Choi D.H. and Kim S.J., 2002, Numerical optimization of the thermal performance of a micro channel heat sink, International Journal of Heat and Mass Transfer, 46(9), pp. 1553-1562.
11. Toh K.C., Chen X.Y. and Chai J.C., 2002, Numerical computation of fluid flow and heat transfer in micro channels, International Journal of Heat Mass Transfer, 45(26), pp. 5133 -5141.
12. Qu W., and Mudawar I., 2002, Experimental and numerical study of pressure drop and heat transfer in a single-phase micro-channel heat sink, International Journal of Heat and Mass Transfer 45(12), pp. 2549–2565.

13. Upadhye H.R. and Kandlikar S.G., 2004, Optimization of micro channel geometry for direct chip cooling using single phase heat transfer, International Conference on Microchannels and Minichannels, June 17-19, Rochester, New York, USA.
14. Hetsroni G., Mosyak A., Pogrebnyak E., and Yarín L.P., 2005, Fluid flow in microchannels, International Journal of Heat and Mass Transfer, 48(10), pp. 1982-1998.
15. Yang C.Y., and Lin T.Y., 2007, Heat transfer characteristics of water flow in micro tubes, Experimental Thermal Fluid Science, 32(2), pp. 432-439.
16. Lelea D., 2009, The heat transfer and fluid flow of a partially heated micro channel heat sink, International Communication in Heat and Mass Transfer, 36(8), pp. 794-798.
17. Zhang S.X., He Y.L, Lauriat G. and Tao W.Q., 2010, Numerical studies of simultaneously developing laminar flow and heat transfer in micro tubes with thick wall and constant outside wall temperature, International Journal of Heat and Mass Transfer, 53(19), pp. 3977- 3989.
18. Satapathy A.K., 2010, Slip flow heat transfer in a semi-infinite micro channel with axial conduction, Journal of Mechanical Engineering Science, 224(2), pp. 357-361.
19. Hasan M.I, 2011, Influence of wall axial heat conduction on the forced convection heat transfer in rectangular channels, Basrah Journal for Engineering Science, 11, pp. 31-43.
20. Moharana M.K., Agarwal G., and Khandekar S., 2011, Axial conduction in single-phase simultaneously developing flow in a rectangular mini-channel array, International Journal of Thermal Sciences, 50(6), pp. 1001-1012.
21. Rahimi M., and Mehryar R., 2012, Numerical study of axial heat conduction effects on the local Nusselt number at the entrance and ending regions of a circular micro channel, International Journal thermal Sciences, 59, pp. 87-94.
22. Moharana M.K., and Khandekar S., 2012, Numerical study of axial back conduction in microtubes, 39th National Conference on Fluid Mechanics and Fluid Power (FMFP2012), 13-15 December 2012, Surat, India.
23. Moharana M.K., Singh P.K., and Khandekar S., 2012, Optimum Nusselt number for simultaneously developing internal flow under conjugate conditions in a square microchannel, Journal of Heat Transfer, 134(7) 071703(1-10).
24. Moharana M.K., and Khandekar S., 2013, Effect of aspect ratio of rectangular microchannels on the axial back-conduction in its solid substrate, International Journal of Microscale and Nanoscale Thermal and Fluid Transport Phenomena, 4(3-4) 1-19.

25. Kumar M., and Moharana M.K., Axial wall conduction in partially heated microtube, 22nd National and 11th International ISHMT-ASME Heat and Mass Transfer Conference, 28-31 December 2013, Kharagpur, India.
26. Tiwari N., Moharana M K. and Sarangi S K., Influence of axial wall conduction in partially heated microtubes, 14th National Conference on Fluid Mechanics and Fluid Power, 12-14 December 2013, NIT Hamirpur, Himachal Pradesh, India.
27. Mishra P., and Moharana M.K., Axial wall conduction in pulsating laminar flow in microtube, 12th International Conference on Nanochannels, Microchannels and Minichannels, FEDSM2014, 3-7 August 2014 Chicago, USA, (Accepted for presentation).
28. Patankar S., 1980, Numerical Heat Transfer and Fluid Flow, CRC Press, USA.
29. Shah R.K., 1975, Laminar flow friction and forced convection heat transfer in ducts of arbitrary geometry, International Journal of Heat and Mass Transfer, 18(7), pp. 849-862.